Levato Lab
FROM SHAPE TO FUNCTION

Scientific Report

CHARACTERIZATION OF A METHOD TO GRAFT BIOLOGICAL MOLECULES INTO NORBORNENE MODIFIED GELATIN HYDROGELS USING VOLUMETRIC PRINTING

Matthias Schweiger (8464510)

Supervision: Riccardo Levato
Daily Supervision: Marc Falandt

Utrecht University | University Medical Center Utrecht

July 20 2022

Universiteit Utrecht

UMC Utrecht

Table of Contents

List of abbreviations

A

ASAP *Ascorbic Acid Phosphate*

D

DOF *Degree of functionalization*
DTT *Dithiothreitol*

E

ECM Extra cellular matrix

F

Fluorescent BSA *Albumin from Bovine Serum-Tetramethylrhodamine conjugate*

G

GelMA Methacrylate modified gelatin
GelNOR *Norbornene modified gelatin*

L

LAP *Lithium Arylphosphinate*

M

MIP-1α *Macrophage Inflammatory Protein 1*α

N

NMR *Nuclear magnetic resonance spectroscopy*

P

PBS *Phosphate buffered saline*
PEG4SH *Poly(ethylene glycol)-tetra-thiol*
PEG-Cy3 *Modified Polyethylene glycol*
PI *Photo-initiator*

R

ROS *Reactive oxygen species*

T

TEMPO *2,2,6,6-tetramethyl-1-piperidinyloxyl*
TNBSA-Reagent *2,4,6-Trinitrobenzene Sulfonic Acid*

V

VBP *Volumetric Bioprinting*

1 Acknowledgements

Hereby I would like to deeply thank Professor Dr. Riccardo Levato for giving me the opportunity to participate in his research group and his angelic patience with me, even though I blew all kinds of deadlines. He gave me the best kind of supervision with the perfect amount of freedom while keeping me on the right path and giving me motivation.

Another important person I want to pay my deepest gratitude is Marc Falandt, who kept on supporting me, not just in a professional way, but a moral as well, even long after I finished my practical work. His practical and theoretical guidance in the laboratory was flawless and, also highly important, he kept on supplying me with memes.

I would also like to thank Professor Dr. Tina Vermonden for providing me with valuable insights and feedback from her department and helping me connect with colleagues beyond our own department.

Another important role in this report played Mattie van Rijen and Anneloes Mensinga. Thank you for the introductions to various instruments, keeping the laboratories in a good shape and also just having an open ear for my many questions during the project.

Final thanks go to Manuel Carro Toregrossa for all the funny lunch breaks, especially in times of the pandemic. You really kept my sanity alive.

To all the ones mentioned above and many more, thank you for turning an internship into a period in my life I will never forget and will always think back to with a smile, despite all hardships.

Matthias Schweiger

2 Abstract

The rapidly emerging scientific field of bio fabrication holds many promises for the production of small body parts, organelles or even whole organs. Needless to say, how big of an impact this would have on the daily life of millions of patients. But with this scientific field being relatively young, certain discoveries and advancements are still to be made. One of the most promising approaches of the research lies in a process, called volumetric bioprinting. Instead of using layer-by-layer printing, this volume-in-volume 3-Dimensional printing method creates a construct within seconds. During this process a mixture of substances, called a bioink, is crosslinked in a volumetric printing process in a volumetric printer. The only impact on the bioink during the crosslinking is light, making the printing a gentle process and therefore highly suited for the printing with living cells. These bioinks predominantly rely on methacrylate-modified gelatin. However, methacrylate-modified gelatin shows to have certain limitations and doesn't allow for further modification, which is needed to create tissues of higher complexity. This report focuses on the synthesis, characterization, and modification of a bioink, which is not reliant on methacrylate. The material used is norbornene-modified gelatin, further on called GelNOR. GelNOR allows for a rapid crosslinking process, making it less susceptible to inhibiting mechanisms compared to methacrylate-modified gelatin. Furthermore, GelNOR hydrogels allow to be modified after crosslinking, utilizing its special crosslinking mechanism. This post-printing modification enables the grafting of biological molecules into the hydrogel. Not only is this new to the field of volumetric bioprinting, but it allows for the spatially controlled printing of specialized tissue by grafting growth factors into the hydrogel. This report is a first step of exploring this promising feature of GelNOR. The first part is focused on the synthesis and analysis of this material, where we could successfully synthesize the material with a high degree of functional groups. Subsequently, the volumetric printing properties of GelNOR were assessed in an approach of optimizing the printing conditions. In this part we optimized the printing resolution of GelNOR by alternating the bioinks composition and the conditions during the printing process. The substances added to the bioink slowed down the crosslinking process, making the printing more modifiable. The third part of this report is focused on the grafting of biological molecules into an already crosslinked GelNOR construct. With various experiments this process was not only proven to be feasible, but it was also shown that, by adjusting the printing conditions to graft the biological molecules, it was possible to spatially control the complex 3-Dimensional designs of the grafted structures inside the printed constructs.

3 Lay Summary

The three-dimensional printing of tissues and even whole organs could solve the needs for millions of patients all around the globe and help to overcome the global donor organ shortage crisis. To reach this goal, the relatively young field of research of biofabrication aims to create scaffolds for cells to thrive in, resulting in functioning tissues and organs. As promising as it sounds, there are still various hurdles to be taken. A lack of variety in the available building materials for these scaffolds and their limitations still hinder this technology from fully exploiting its potential. An example for such a limitation is that most materials cannot be modified, after the scaffold was printed. However, this is essential for the creation of tissues or organs of higher complexity. The reason for this is that complex organs are comprised of various different and specialized cell types, and the functionality of these organs is dependent on their correct spatial arrangement. Conventional scaffold-printing materials don't have a control mechanism to arrange specialized cell types. In the human body, biologically active molecules cause stem cells to transform into specialized cell types. This report is focused on the characterization of a method to attach such biologically active molecules into already printed scaffolds, using a special scaffold material. The method of attaching these molecules is the same as for constructing the scaffolds. After proving the possibility of such a modification, it was even possible to attach them in a spatially controlled arrangement. This lays the foundation of printing tissues and organs of higher complexity and bares the potential of being a quantum leap in the field of biofabrication, as this has never been done before. Building upon the findings in this report, further research remains to be done, in order to bring this promising technology to patients' use. It is hard to predict, when this technology will be available for clinical application, but the impact it will be undeniably huge.

4 Introduction

4.1 Biofabrication

Biofabrication is a scientific field, specializing on the fabrication of functional tissues and can be understood as a combination of biology, engineering and material science. The fabricated constructs are designed to have a biological structural organization. This means, that the basic building materials are of biological origin and biocompatible. Further, the application of bioactive molecules and even the inclusion of living cells or cell aggregates are desirable (1). An important aspect of biofabrication techniques is to adequately mimic the conditions of the native tissues and organ structures (2). This is can be achieved by creating a biocompatible scaffold, which allows for the proliferation of cells and the transport of nutrients, but also shows biodegradability (3). A common approach for this is a technology called bioprinting. Hereby, a substance called bioink is processed to form scaffold structures for cells to thrive in. A bioink essentially entails a mixture of compounds that can be processed by an automated biofabrication technology, that is containing cells and optionally biologically active components (4). Although this has been done in a two-dimensional scale, the fabrication processes for three-dimensional structures with appropriate conditions remain to be developed and refined (2). To fabricate these three-dimensional structures, bioprinting is combining the principles of tissue engineering and 3D-printing. The most common understanding of the process of 3D-printing is the extrusion-based additive layer-by-layer processes. An example of these processes is inkjet-printing [Figure 1A], where single droplets of bioink are dispensed on a building platform and subsequently crosslinked. This method requires the bioink to have a lower viscosity than other extrusion-based processes. Li et al. used alginate as a basic material for their inkjet-printing bioink and could refine this process to reach a drop size of just tens of micrometers (5). Another extrusion-based layer-by-layer method is microextrusion [Figure 1B]. Microextrusion comprises a steady bioink flow using air pressure, piston- or screw-assisted extrusion systems. Like inkjet-printing, microextrusion requires the bioink to have a low viscosity. However, Kim et al. developed a printing strategy to apply low-viscosity bioink, based on fibrinogen, in a high resolution by printing on a micro structured substrate to hold the bioink in place during printing (6). A printing process using a laser to apply bioink on a surface in a layer-by-fashion is laser-assisted bioprinting [Figure 1C]. Hereby, the building material is applied on a substrate surface by projecting a laser beam onto an energy absorbing layer. This causes the absorbing layer to evaporate, resulting in high-pressure bubbles of microscopic scale between the side of the absorbing layer, which faces the bioink, and the substrate surface. These microscopic high-pressure bubbles create a jet of material towards the substrate surface (7). Unlike other 3D-printing methods, laser-assisted bioprinting requires a high-viscosity bioink. As stated by Dou et al., laser-assisted

bioprinting can print with a high resolution up to the scale of microns. Commonly used bioinks for laser-assisted bioprinting are based on gelatin (8).

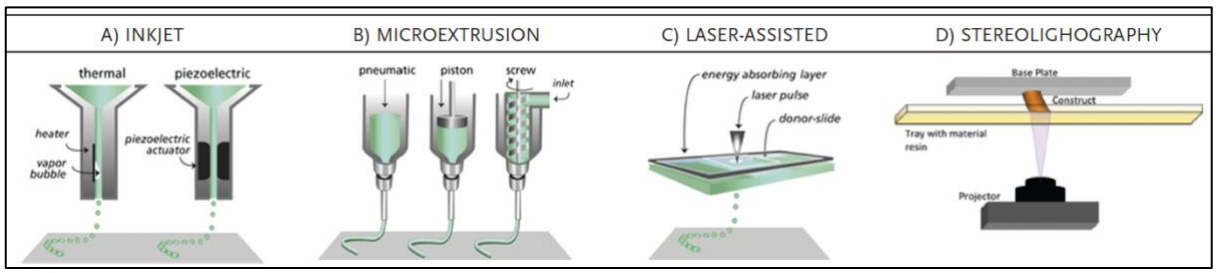

Figure 1: 4.1 Biofabrication – *Schematic of layer-by-layer methods of 3-Dimensional printing. A: Inkjet printing, B: Microextrusion based printing, C: Laser-assisted printing and D: Stereolithography (7).*

Next to the application method of the bioink, the mechanism of how the bioink is crosslinked plays an important role in the process development, as it does not only determine the mechanical properties of the bioink, but also the impact on the cells, encapsulated within the bioink. Examples of crosslinking mechanisms is thermal gelation, pH, ionic, enzyme-based crosslinking or photopolymerization (2). A special crosslinking method to be mentioned is photopolymerization (light-induced crosslinking) as it allows for a clean spatially and temporally controlled crosslinking. The commonly used spectrum of light ranges from ultra violet to visible light. However, using visible light shows to have a higher cell compatibility and results in more uniform structures, since it has a higher penetration depth. To make use of this crosslinking mechanism, the bioink has to contain a photo-initiator (PI) or has to be based on a photoresponsive polymer. Upon the impact of light, the PI generated free radicals by homolytic bond cleavage, which induces the bioinks respective polymerization mechanism (9). A layer-by-layer process, making use of such a photo crosslinking mechanism is stereolithography [Figure 1D]. During this printing process, a printing platform is submerged into the bioink and a complete layer crosslinked onto the platform/previous layer. This is achieved by projecting light into the printer's polymerization plane within the bioink with a projector, inducing the crosslinking of a new layer onto the platform/previous layer. A problem of this process is the unwanted mixing of materials, when switching between different bioinks. To overcome this, Grigoryan et al. developed a multi-material printer minimizing the mixing of materials. An example of bioinks, Grigoryan et al. used, is methacrylated hyaluronic acid mixed with the photo-initiator Lithium Arylphosphinate (LAP) (10).

However, all of the printing techniques mentioned above show significant disadvantages. Extrusion-based methods show a significant shear stress, applied on the bioink, reducing cell viability (11). Another limitation of the fabrication of biologically functional products with layer-by-layer methods is the slow pace of the process. A slow printing process results is a high stress for the cells within the bioink during printing. Therefore, the size-scalability of printable constructs with cell-laden bioinks is limited, as the printing time exceeds 1 hour or more, when printing in a scale of just centimeters (12). These

limitations show the necessity and requirements for a more suitable, rapid and cell conserving printing method.

4.2 Volumetric bioprinting

A nozzle-free method to fabricate whole structures instantly is Volumetric bioprinting (VBP). VBP surmounts the disadvantages of common layer-by-layer methods, as the bioink is not applied through a nozzle, therefore bypassing shear-forces. The technology allows for a rapid printing process of high spatial precision, resulting in an exceptionally high cell viability. Hence, VBP is a promising approach revolutionize future medicine. As an example, Gehlen et al. printed centimeter scaled constructs with micrometer scaled resolution within printing times of under 1 minute. Additionally, these constructs showed a high cell viability, proving the enormous potential of this technology (13). The method makes use of radical-induced photopolymerization in the visible light spectrum as a crosslinking mechanism. During the printing process, the bioink is placed in a rotating container [Figure 2]. A laser projects a DLP-modulated set of 2-Dimensional images of the construct to be printed into the rotating vial, containing the bioink. The set of 2-Dimensional images comprises of individual images of a 3-Dimensional object from different angles. The consecutive sequence of 2-Dimensional images results in rotating 3-Dimensional image being projected into the bioink. The rotation speed of the 3-Dimensional image matches the speed of the rotating vial with the bioink. This emanates in a spatial accumulation of light impact, where crosslinking is desired. If the accumulated light dose exceeds a certain threshold, the polymerization process starts. An overexposure leads to polymerization processes in undesired spatial regions, making the light dose an essential component of this method. The printing process can be observed with a camera, which is facing the rotating vial in a 90° angle from the projection (12).

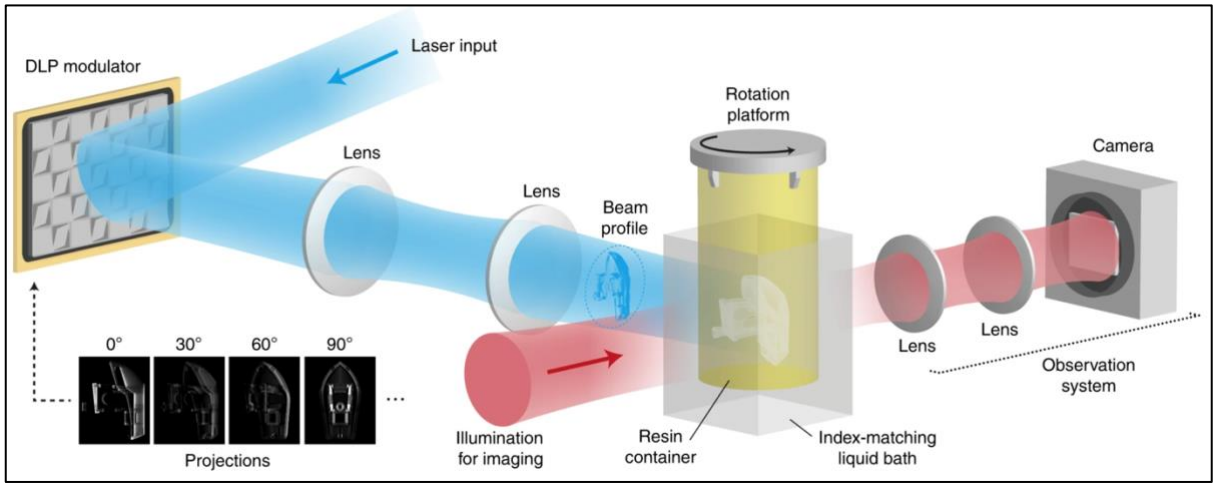

Figure 2: 4.2 Volumetric bioprinting – *Schematic of the volumetric printing method. A modulated laser input is projected into a rotating resin container, inducing the polymerization process. The process can be observed with a camera (14).*

To ensure the processability of a bioink, it needs to contain a substance that serves as a matrix for the cells after the printing process. A commonly used substance for this purpose is methacrylate modified gelatin (GelMA), as it closely mimics the extracellular matrix (ECM). GelMA is synthesized by reacting gelatin with methacrylic anhydride, resulting in the substitution of the reactive amine and hydroxyl groups of the gelatin with methacrylol groups [Figure 3](15).

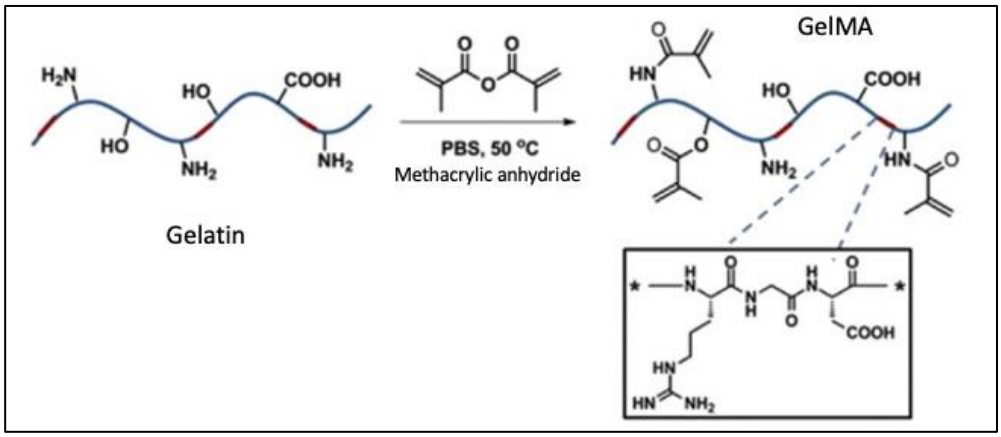

Figure 3: 4.2 Volumetric bioprinting - *Schematic of GelMA synthesis reaction. Reactive amine and hydroxyl groups on the backbone of the gelatin react with methacrylic anhydride at 50°C and form GelMA (15).*

GelMA can be printed with negative and/or positive features in a high resolution and with the addition of certain substances to the bioink, a high concentration of living cells can be added to the bioink during the printing process without reducing the printing resolution. Bernal et al. give a good example of such a tuning process of GelMA. Bernal and her team faced the problem of light scattering, caused by the cells/organoids within the bioink, leading to reduced printing resolution. By adding the biocompatible compound iodixanol to the bioink, Bernal et al. adjusted the refractive index of the GelMA based bioink to match the refractive index of the embedded cells/organoids. This drastically reduced the light scattering, while maintaining a high cell viability (16).

Despite all these promising features, GelMA shows limitations. The crosslinking mechanism of GelMA is free-radical chain growth and, as all radical induced growth mechanisms, susceptible to oxygen inhibition (17). In short, the crosslinking process starts with the initiation step: the light exposure induces the dissociation of the PI into radicals, causing the methacrylol groups of the GelMA to form radicals. The following is the propagation step: The methacrylol radicals react with each other by forming a covalent bond and thereby building a network. The reaction is eliminated by 2 radicals reacting with each other or the depletion of PI (18). The inhibition mechanism is caused by the high affinity of molecular oxygen to the radical activated methacrylol groups of the GelMA (19). Oxygen inhibition can cause various effects on the bioink, such as slowing down polymerization rates and prolonging induction periods (20). Another harmful effect is the formation of reactive oxygen species (ROS), which has a negative impact on the viability of the encapsulated cells

in the bioink (21). Further on, GelMA doesn't allow for further modification after the printing process, such as the application of bioactive molecules. This is due to the depletion of reactive groups during the crosslinking process. Another limiting factor of GelMA is the lack of control over the hydrogel stiffness and mechanical properties. As many advantages volumetric bioprinting with GelMA holds, as many limitations it has when it is to be used for the fabrication of complex structures and tissues. To overcome these limitations and to further propel the advancement of (volumetric) bioprinting, a higher diversity in the selection of biomaterials is essential (22).

4.3 GelNOR

A promising candidate for overcoming the limitations of GelMA is norbornene modified gelatin (GelNOR). The reaction of the GelNOR synthesis is based on the gelatin's primary amines, functioning as a nucleophile for the carbic anhydride. This S_N2 nucleophilic substitution reaction results into an amide bond between the norbornene moiety and the gelatin derived backbone of the polymer [Figure 4]. The degree of norbornene functionalization of the lysine count in the gelatin can be modified by adjusting the pH, the amount of carbic anhydride, the temperature of the reaction solution, or the time of the reaction (23).

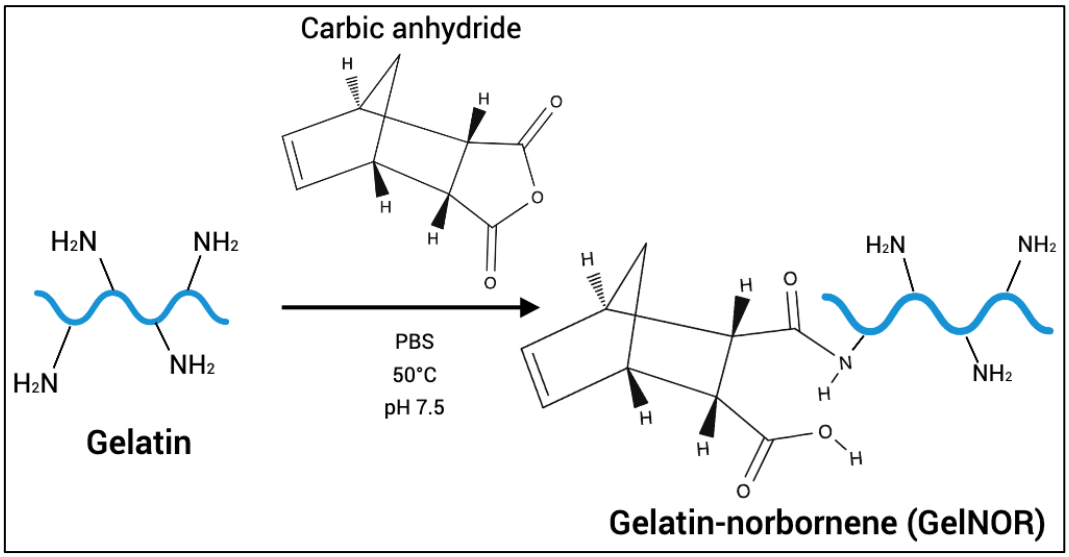

Figure 4: 4.3 GelNOR – *Schematic of GelNOR synthesis reaction. Gelatin reacts with carbic anhydride at 50°C and pH 7.5 and forms GelNOR in a nucleophilic substitution reaction.*

The crosslinking mechanism of GelNOR is based on a radical-mediated step-growth thiol-norbornene photoclick reaction. The initiation step during this process is the exposure of a PI to visible light, causing the generation of free radicals [Figure 5A]. These radicals cause the radicalization of a thiol-containing molecule [Figure 5B]. This thiol-radical reacts with the C=C bond of a norbornene modified gelatin or another macromer, resulting in a covalent thiol-bridge. The radical character causes the radical formation of another thiol-group, thereby propagating the reaction. The elimination mechanism is the same as for GelMA (24).

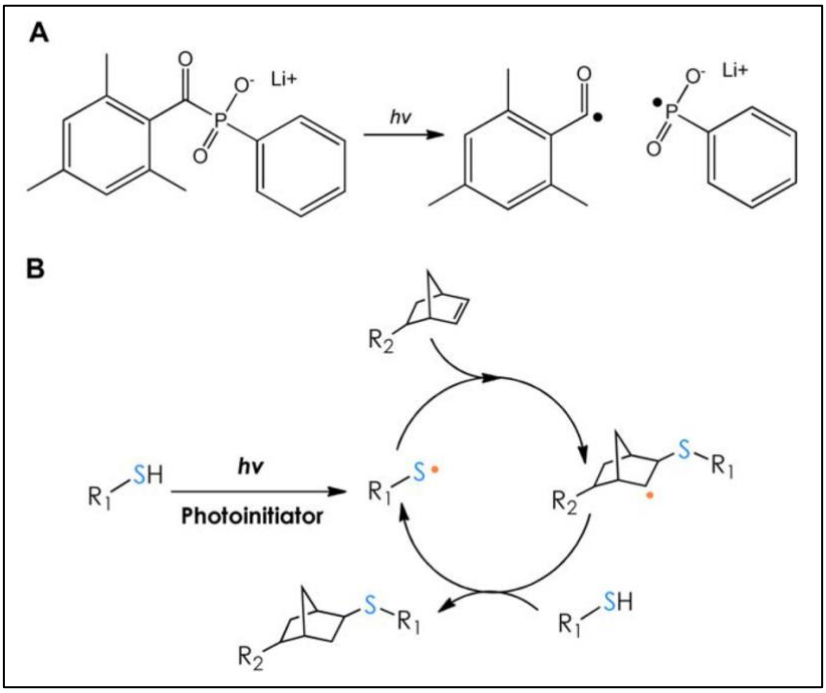

Figure 5: 4.3 GelNOR – *Schematic of the radical-mediated step-growth thiol-norbornene photoclick reaction mechanism. A: Visible light induces the disintegration of the PI (LAP in this schematic) into radicals. B: The PI radical causes the radicalization of a thiol, which forms a covalent bond with a c-c double bond involved carbon atom of the norbornene group. This causes the other carbon atom of the c-c double bond to have a radical character, which causes another thiol to radicalize (24).*

The step-growth crosslinking mechanism of GelNOR has several advantages over the chain-growth mechanism of GelMA. The reactions fast pace leads to a significantly lower sensitivity to oxygen inhibition (21). GelNOR can be used in lower polymer concentrations what causes the printed construct to be more permissive. Another advantage is the high efficiency of the crosslinking, reducing the needed amount of modified groups within the gelatin, hence preserving its native character. Furthermore, the mechanical properties can be easily controlled by the choice and amount of crosslinker added to the bioink. In addition, GelNOR allows for the formation of homogeneous networks with reduced shrinkage and mechanical stress. The biggest advantage of GelNOR over GelMA is most likely the possible application of bioactive molecules into the hydrogel. This is possible, as the crosslinking mechanism of GelNOR allows for preserving reactive groups within the hydrogel, providing them for further modification (25).

As all radical induced crosslinking mechanisms, the crosslinking of GelNOR can be controlled by the addition of an inhibiting substance to the bioink in order to prevent fast polymerization in unwanted regions and therefore increase the printing resolution, as described by Rizzo et al. (25). An example for these inhibiting substances is ascorbic acid and they serve the purpose of scavenging the radicals, therefore providing a higher tunability of the polymerization process (26). The crosslinking reaction kinetics of GelNOR show a high level of controllability by varying the degree, of which the gelatins primary amines have been substituted with norbornene groups during the synthesis (Degree Of Functionalization, DOF).

The DOF correlates directly with the hydrogel stiffness, where a higher DOF makes for a stiffer hydrogel. The structure of the thiolated crosslinkers also plays a role in the pore-size and stiffness of the printed GelNOR constructs (25). For this report, the thiol containing molecule in the bioink is Dithiothreitol (DTT) [Figure 6]. As it contains two thiol groups, the DTT in the bioink reacts with two norbornene groups and thereby serves as a bridge between macromers during the crosslinking.

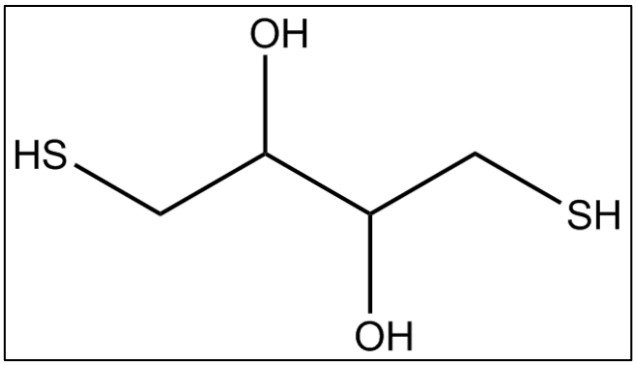

Figure 6: 4.3 GelNOR – *Schematic of the used crosslinker molecule DTT (27)*

Another factor of the GelNOR hydrogels properties is the ratio of thiol-groups to norbornene-groups in the bioink. A thiol-norbornene ratio of 1:1 result in the stiffest hydrogels. However, as indicated by Rizzo et al., a different ratio gives the possibility of further functionalization steps (25). The theory here is to utilize a free cysteine rest (thiol-group) of an amino acid within a protein to bind it onto the norbornene groups of GelNOR, which did not react during the crosslinking. The reaction mechanism is the same as the crosslinking process of the GelNOR, whereby the LAP radical promotes the forming of a thiol-bond between a norbornene group of the hydrogel and the cysteine rest of a protein. To have free norbornene groups within the hydrogels, we crosslinked the cylinders with a DTT concentration of approximately 70% saturation of norbornene groups. This would immensely widen the applications of GelNOR, as it would enable the application of e.g., growth factors into hydrogels. The spatially controlled application of growth factors into hydrogels could give way for the controlled differentiation of stem cells within the bioink, resulting in a complex tissue comprising various types of different cells.

Rizzo et al. conducted thorough research on GelNOR in a large set of experiments, where they could characterize the correlation between the mechanical properties of the GelNOR constructs and varying DOFs, different crosslinkers and GelNOR concentration. These results showed, that the higher the DOF, the amount of thiol groups within a crosslinker molecule and the GelNOR concentration, the stiffer the GelNOR print. Further on, they could prove the printability of GelNOR constructs with a high shape fidelity in centimeter-scale as well as in micrometer-scale [Figure 7] (25).

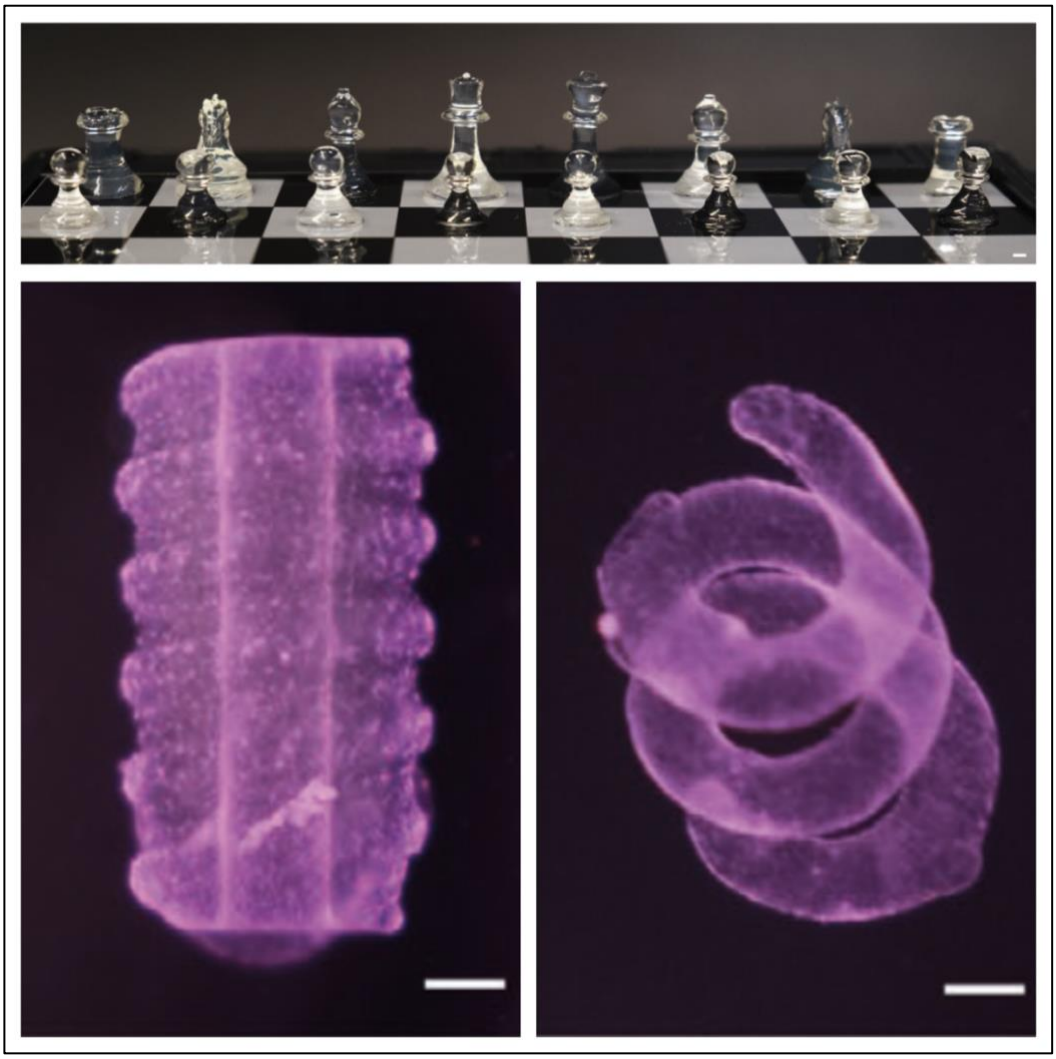

Figure 7: 4.3 GelNOR – *Illustrations of GelNOR constructs fabricated by Rizzo et al. Top: a set of chess figures printed with 5% w/v GelNOR; scalebar: 2mm. Bottom: two spiral like constructs, printed with 2.5% w/v GelNOR; scalebar: 2mm (25).*

The research on GelNOR by Greene et al. showed a high cell viability under similar fabrication conditions. The difference in the experimental settings is the crosslinker molecule. Greene et al. utilized poly(ethylene glycol)-tetra-thiol (PEG4SH) [Figure 8] (28).

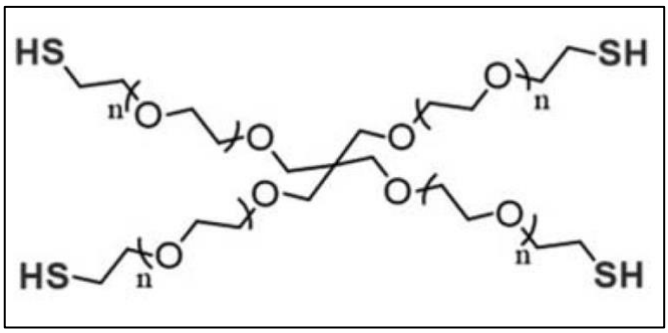

Figure 8: 4.3 GelNOR – *Schematic of poly(ethylene glycol)-tetra-thiol, the crosslinker used by Greene et al. to assess the cell viability of GelNOR (28)*

A study by Göckler et al. utilized a second gelatin macromer as a crosslinker to fabricate GelNOR hydrogels. The second gelatin macromer was modified by chemically attaching thiol groups onto the gelatin's backbone. The utilization of such a crosslinker resulted in an incredibly rapid polymerization process within 1-2 seconds (29). By utilizing a lithography-based 3D-ptinting method, Dobos et al. fabricated GelNOR hydrogels with a high resolution in the range of micrometers (30) showing the versatility of this material.

4.4 Aims of the report

This report aims to explore the possibilities of GelNOR in order to widen the possible applications for this bioink. Therefore, this report is divided into several segments: The first experiments aim to synthesize and characterize GelNOR and to test the functionality by analyzing the polymerization properties and the DOF after synthesis in a higher DOF than in previously published works. Because of the higher DOF the GelNOR will be better suited for engrafting possibilities and variation in crosslinker densities, utilizing the versatility of the material. The second part of this report is focused on the crosslinking process of GelNOR and the optimization if its printing conditions by testing various compositions of the GelNOR bioink, printing conditions and the addition of a photo inhibitor in order to modulate the polymerization process. In the third part, the focus will be on the grafting of biological molecules into crosslinked GelNOR constructs by utilizing free norbornene groups and the optimization of this process. This step will lay the foundations of the spatially controlled printing of specialized tissue, thereby giving control over the tissues biological function, causing a paradigm shift within biofabrication and VBP.

5 Materials and methods

The used gelatin (Porcine type A) was purchased from Rousselot. Carbic anhydride was purchased at Acros Organics. DTT, 2,2,6,6-tetramethyl-1-piperidinyloxyl (TEMPO), 2,4,6-Trinitrobenzene Sulfonic Acid (TNBSA-Reagent) and the cellulose membrane dialysis tube (cutoff = 12 kDa) were purchased from Sigma-Aldrich. Glycine, sodium bicarbonate and LAP was purchased from Merck. Albumin from Bovine Serum-Tetramethylrhodamine conjugate (Fluorescent BSA) was purchased at Thermo-Fisher. The freeze-drying device Alpha 1-4 LSCbasic was purchased from Christ. The volumetric 3D-printer Tomolite was purchased from Readily3D. The microscope BX51 was purchased from Olympus. The Thunder microscope was purchased from Leica.

The used methods are listed under each experiment individually.

5.1 Synthesis and characterization of GelNOR

5.1.1 Gelatine norbornene synthesis

Porcine gelatin type A (10g) was dissolved in preheated 50°C PBS (90 mL). The mixture was stirred at 50°C until the gelatin was completely dissolved. Subsequently, carbic anhydride (18 g, 109.6 mmol) was slowly added to the reaction mixture. 5 M NaOH was added to the reaction mixture to assure the dissolvement of carbic anhydride. Afterwards the pH of the mixture was stabilized to 7.5 with 5 M NaOH and 6 M HCl. The reaction mixture was left stirring at 50°C for 24 h in the dark.

Next, PBS (180 mL) was added to the reaction mixture. The mixture was centrifuged at 4000 rpm for 5 minutes at room temperature. The combined supernatant was dialyzed against deionized water for 7 days at 4°C, changing the deionized water twice a day. Subsequently, the solution was sterile filtered with 0.22 µm filter, frozen at -80°C and lyophilized. The dried GelNOR was stored at -20°C.

5.1.2 TNBS Assay

As calibration curve, a Glycine stock solution (c = 10 mM) was prepared in the reaction buffer (0.1 M Sodium Bicarbonate [$NaHCO_3$] pH=8.5). A serial dilution of the glycine stock (c = 10 mM) provides the calibration solutions of the following concentrations: 0.5 mM, 0.3 mM, 0.25 mM, 0.2 mM, 0.15 mM, 0.1 mM, and 0.05 mM. The standard curve for calibration was measured in duplicates. For the GelNOR and gelatin stock solutions the materials were dissolved in reaction buffer at a concentration of 1 w/v%. The sample and reference stock solution were diluted with reaction buffer to provide the following concentrations: 0.09 w/v%, 0.06 w/v% and 0.045 w/v%. The GelNOR and gelatin measurements were performed

in triplicates. The TNBSA Reagent (c = 5 w/v% in H_2O) was diluted with Milli-Q water to a concentration of 0.01 w/v%. Each stock solution (300 µl) was mixed with the TNBSA reagent (200 µl) in a 96-Well plate and incubated for 30 minutes at room temperature protected from light. Afterwards the absorbance was measured in a UV-Vis plate reader at λ=335 nm.

5.1.3 Hydrogel casting

For this experiment, a 10 w/v% GelNOR solution containing 0.05 w/v% LAP and 10 mM DTT were casted in a silicone mold, forming biconvex lenses of approximately 4 mm in diameter and crosslinked in an UV-oven for 10 minutes (λ = 365 nm). Subsequently, the discs were optically assessed and the rigidity tested with a spatula.

5.2 Optimization of the printing conditions

For this experiment, a solution of 10 w/v% GelNOR, containing 0.05 w/v% LAP, was produced with varying concentrations of DTT and the photo inhibitor Ascorbic Acid Phosphate (ASAP) [Table 1]. The bioink was loaded into the printing vial and subsequently placed in an ice bath, protected from light, to ensure thermal gelation of the gelatin-based bioink. Afterwards, a 3-Dimensional structure was printed with the bioink in the volumetric printer, forming a hydrogel complex. The printing conditions varied for each hydrogel in time of light exposure (dose = mJ/cm^2) and light intensity (mW/cm^2) [Table 1]. After the printing process, the vial was washed with 37°C PBS to remove the non-crosslinked hydrogel. Subsequently the channel in the printed hydrogel was flushed with air using a pipette. Every material or reagent was dissolved in PBS unless stated differently.

Hydrogel number	Concentration DTT [mM]	Concentration ASAP [w/v%]	Time of light exposure [s]	Light intensity [mw/cm^2]
1	8	0	120	5.8
2	8	0	112	4
3	8	0	110.5	4
4	8	0.01	112	4
5	8	0.01	118.5	4
6	8	0.001	118.5	4
7	8	0.005	118.5	4
8	8	0.005	110.5	4
9	8	0.001	110.5	4
10	8	0.005	114.5	4
11	6	0.001	110.5	4
12	6	0	91	5
13	6	0	92	5

Table 1: 5.2 Optimization of the printing conditions - *Overview of the different hydrogel compositions and printing conditions. All hydrogels had a GelNOR concentration of 10% w/v and 0.05% w/v LAP.*

5.3 Grafting of biological molecules into GelNOR

10.7 mg of 2,2,6,6-tetramethyl-1-piperidinyloxy (TEMPO) was dissolved in 2675 µl ethanol to reach a 0.4 w/v% TEMPO stock solution. For the stock solution of the modified Fluorescent-BSA, 5 mg was dissolved in 2.6 ml PBS. To produce the stock solution of 0.1 w/v% modified Polyethylene Glycol (PEG-Cy3)(5 kDa), bound to a fluorescent dye and a Thiol-group, 50 mg of PEG-Cy3 was solved in 50 ml PBS. For the 2.5 w/v% stock solution of LAP, 375 mg of LAP was dissolved in 15 ml PBS. All materials or reagents were dissolved in PBS unless stated differently.

A Solution of 5 w/v% GelNOR was crosslinked with 4.2 mM DTT and 0.05 w/v% LAP for 15 minutes in an UV-oven into cylinders with a diameter of 8.1 mm. Subsequently, the cylinders were cut to a length of 2.9 cm and washed in PBS for 12 hours at 4°C. These GelNOR cylinders were used in the following experiments.

5.3.1 Grafting feasibility

6 GelNOR cylinders were infused with variations of an infusion mix (1.25 ml), containing TEMPO, LAP, BSA and PBS. The infusion mix had a concentration of 0.19 w/v% BSA (equals a concentration of approximately 0.03 mM), with concentrations of 0.5 and 1 w/v% LAP, and 0, 0.006 and 0.012 w/v% TEMPO [Table 2].

Cylinder number	Concentration LAP [w/v%]	Concentration TEMPO [w/v%]
1	0	0
2	0.5	0
3	1.0	0
4	0.5	0.006
5	1.0	0.006
6	0.5	0.012
7	1.0	0.012

Table 2: 3.3.1 Disc printing – *Overview of the different infusion conditions of the GelNOR cylinders for the grafting feasibility experiment. The cylinders had a GelNOR concentration of 5% w/v and were infused with an infusion mix, containing 0.19% w/v fluorescent BSA.*

A cylinder without LAP and TEMPO was prepared as a blank. The infusion process took place for 90 minutes in the dark at 4°C. After the infusion, the cylinders were loaded in a printing vial and placed in a volumetric printer. Subsequently, discs of 6 mm in diameter and 1 mm in height were projected into the GelNOR cylinders. The light dose of the discs was 150-, 200-, 250-, 300-, and 350 mJ/cm^2 from bottom to top (vertically) for each cylinder [Figure 9].

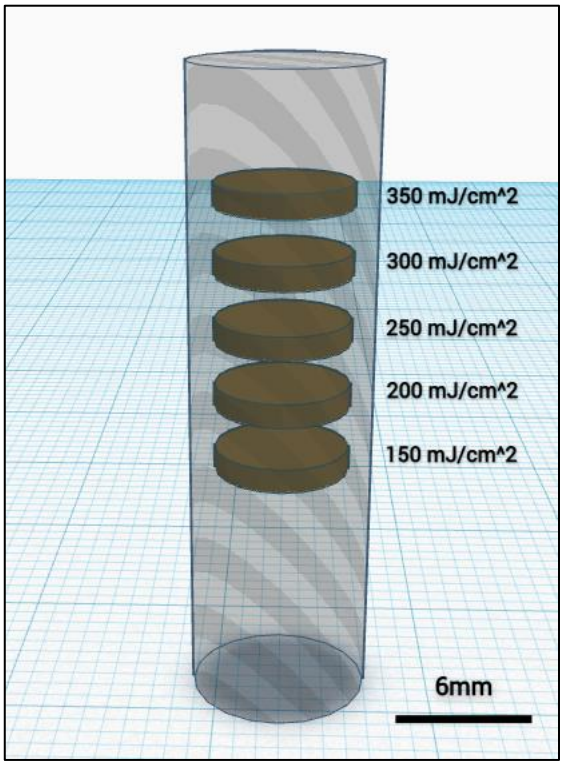

Figure 9: 5.3.1 Grafting feasibility – *Schematic of the grafted discs (brown, 6mm in diameter) within the GelNOR cylinders and their corresponding light doses. The light dose, used to graft the discs into the GelNOR cylinder with fluorescent BSA, decreased from top to bottom.*

After the printing process and washing the cylinders for 24 hours in PBS at 4°C in the dark, the cylinders were frozen at -20°C for 15 minutes. Following, the vertical central cross-section, with a thickness of 1.3 mm, was cut out the cylinders and analyzed under the microscope. The assessment of the cross-sections was performed with an Olympus IX53 fluorescent microscope under the exposure of green light (λ=560 nm).

5.3.2 Grafting optimization

In the following experiments, PEG-Cy3 was used as a fluorescent dye for the infusion mix with a concentration of 0.05 w/v%. The infusion- and printing conditions of the GelNOR cylinders are listed under each experiment individually. The infusion process for the following experiments took 90 minutes at 4°C in the dark. The infused cylinders were loaded into printing vials and the various structures printed. Subsequently, the GelNOR cylinders were washed in PBS (4°C) for 24 hours in the dark. After the washing, the cylinders were shock frozen in liquid Nitrogen for approximately 20 seconds and the vertical cross-sections were cut out to reach a thickness of 1.3 mm. The pictures, acquired with the Thunder microscope, were later on analyzed with ImageJ.

The cylinders for the first experiment were infused with a concentration of 0.6, 0.8 and 1.0 w/v% LAP and 0.006, 0.008 and 0.010 w/v% TEMPO [Table 3].

Cylinder number	Concentration LAP [w/v%]	Concentration TEMPO [w/v%]
1	0	0
2	0.6	0.006
3	0.6	0.008
4	0.6	0.010
5	0.8	0.006
6	0.8	0.008
7	0.8	0.010
8	1.0	0.006
9	1.0	0.008
10	1.0	0.010

Table 3: 3.3.1 Disc printing – *Overview of the different infusion conditions of the GelNOR cylinders for the grafting optimisation. The cylinders had a GelNOR concentration of 5% w/v and were infused with an infusion mix, containing 0.05% w/v PEG-Cy3.*

The printed constructs, discs of 6 mm in diameter and 1 mm in height, were printed in each cylinder with a light dose of 750-, 1000-, 1250-, 1500-, 1750-, and 2000 mJ/cm^2 in a volumetric printer [Figure 10].

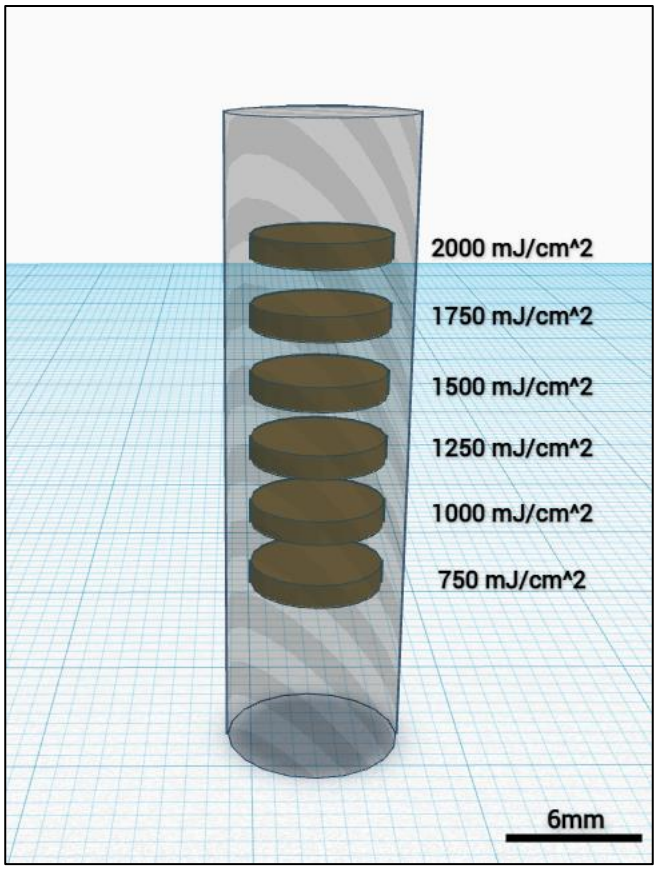

Figure 10: 5.3.2 Grafting optimization - *Schematic of the grafted discs (brown, 6mm in diameter) within the GelNOR cylinders and their corresponding light doses. The light dose, used to graft the discs into the GelNOR cylinder with PEG-Cy3, decreased from top to bottom.*

In the following experiment, the infusion mix had a concentration of 0.8 and 1.0 w/v% LAP and 0.007, 0.008 and 0.009 w/v% TEMPO [Table 4].

Cylinder number	Concentration LAP [w/v%]	Concentration TEMPO [w/v%]
1	0.8	0.007
2	0.8	0.008
3	0.8	0.009
4	1.0	0.007
5	1.0	0.008
6	1.0	0.009

Table 4: 3.3.2 Two dimensional fractals - *Overview of the different infusion conditions of the GelNOR cylinders for the fractal printing. The cylinders had a GelNOR concentration of 5% w/v and were infused with an infusion mix, containing 0.05% w/v PEG-Cy3. The fractals were grafted with a light dose of 2000 mJ/cm².*

Two fractals were printed above each other with a light dose of 2000 mJ/cm^2 for the lower and 4000 mJ/cm^2 for the upper fractal in a volumetric printer.

In the following, a three-dimensional object was grafted into GelNOR cylinders after infusing the hydrogel cylinders with a concentration of 1.0 w/v% LAP and 0.008 w/v% TEMPO. The object was printed with a light dose of 2000 mJ/cm2 in a volumetric printer. After the printing process and washing the cylinders for 24 hours in PBS at 4°C in the dark, the hydrogel cylinders were stored in the dark in PBS, containing 0.05 w/v% sodium azide until image acquisition. The acquisition of the images was not performed in our laboratory.

6 Results and discussion

6.1 Synthesis and characterization of GelNOR

6.1.1 Gelatin norbornene synthesis

Optically, the synthesis protocol resulted in a white substance with a stiff, foam like structure. This was the case throughout all the produced batches of GelNOR. However, further testing of the crosslinking properties of the synthesized GelNOR indicated the necessity of a second dialysis step, caused by the presence of carbic anhydride in the synthesized material. This will be further investigated and discussed in the following experiment sections. Nevertheless, the synthesis was successful for every batch.

6.1.2 TNBS Assay

The TNBSA Assay was performed to determine the DOF of the synthesized gelatin norbornene material. With this assay, the amount of free amine groups is measured, where the gelatin stock, used in the synthesis of the material, is utilized as a reference for the gelatin norbornene material. The assays principle is the binding of the TNBSA reagent onto the free amine groups of the gelatin's lysine, forming an orange complex which is measured in an UV/VIS-Photometer [Figure 11].

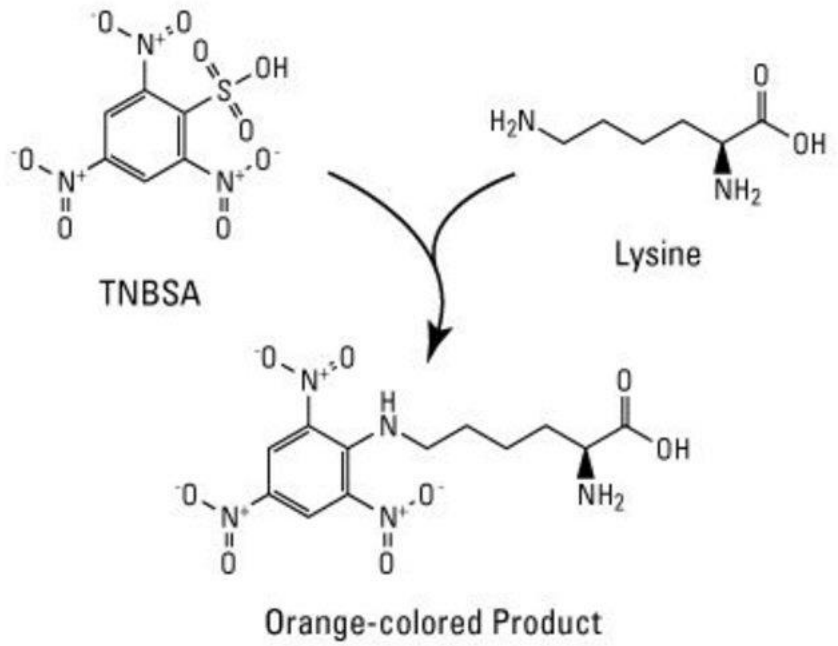

Figure 11: 6.1.2 TNBS Assay – *Schematic of the TNBS Assay detection principle. The free amine group of a lysine reacts with the TNBSA agent and forms an orange-colored product that can be measured in a UV/Vis-plate reader (31).*

The calibration curve for the TNBS assay was determined by a linear regression of the arithmetic means for the duplicates and their corresponding concentration. Hereby, the x-axis plots the glycine concentration and the y-axis the absorbance.

To calculate the amount of lysine groups in the gelatin reference and GelNOR samples, the arithmetic means of the triplicates for each sample's concentration was divided by the calibration curve's slope and subtracted by the calibration curve's offset [Equation 1].

Equation 1: 6.1.2 TNBS Assay – *Formula to calculate the Lysin concentration based on absorbance*

$$c(Lysin)\ [mM] = \frac{Arithmetic\ mean\ of\ Absorbance\ triplicate}{Slope} - Offset$$

The final calculation for this experiment was to assess the degree of functionalization. Therefore, the ratio between the lysin concentration of the GelNOR and the gelatin reference is subtracted from 1 and multiplied by 100 (32) [Equation 2].

Equation 2: 6.1.2 TNBS Assay – *Formula to calculate the degree of functionalisation*

$$Degree\ of\ functionalisation\ [\%] = (1 - \frac{c(Lysin)GelNOR}{c(Lysin)Gelatin}) * 100$$

The calculated values for DOFs can be seen in Table 5. The average value for the DOF of the synthesized batches is 87.8% with a relative standard deviation of 4.2%. Despite the sample size being rather low (n = 4), the synthesis protocol with a relative standard deviation of below 5% can be considered reproduceable.

	GelNOR Batch1	GelNOR Batch2	GelNOR Batch3	GelNOR Batch4
Degree of functionalization [%]	92.2	90.7	84.3	84.0

Table 5: 6.1.2 TNBS Assay – *Calculated DOFs for the synthesized GelNOR batches. The calculations are based on the data, retrieved with the UV/Vis-plate reader during the TNBS assay.*

To calculate the concentration of norbornene groups of the GelNOR, the lysin concentration of each GelNOR sample was subtracted from the lysin concentration of the corresponding gelatin reference [Equation 3]. The necessary data for these calculations were acquired with the TNBSA assay.

Equation 3: 6.1.2 TNBS Assay – *Formula to calculate Norbornene groups of GelNOR*

$$c(Norbornene\ groups)[mM] = c(Lysin)Gelatin - c(Lysin)GelNOR$$

We expected the DOF to be around 40-50%, since the experiments, carried out by Mũnoz et al., 2014 under similar conditions, gave results in this range of DOF (23). The mentioned synthesis experiments by Mũnoz had almost identical concentrations of chemicals to the synthesis protocol of this report. The only concentration difference was the concentration of gelatin (10% w/t for the Mũnoz protocol and 11.1% w/t in this report). Mũnoz and his team had a range of conditions for the synthesis in terms of pH and reaction time, ranging from pH 8 to 9 and reaction times between 2 and 70 hours. However, the reaction time in this protocol was well within the tested range by Mũnoz et al. and the pH of the reaction solution did not differ significantly. We therefore expected the DOF to be within the same range. The reason for the big difference in DOF remains to be determined. However, Göckler et al. were able to synthesize GelNOR with a DOF >95%, using a different synthesis protocol. Göckler and his team used 5-Norbornene-2-carboxylic acid as a source of norbornene groups and converted it into a succinimidyl ester before starting the substitution reaction with the gelatins lysin groups (29). This procedure might be applicable for a modification of the synthesis protocol in this report to further increase the DOF.

A possible way to reevaluate the DOF could be a second assay with a higher concentration of the GelNOR samples, as the absorbances of these samples were below the general linear range of photometers of 0.1 – 1 (33). Another method to confirm the DOF is nuclear magnetic resonance spectroscopy (NMR). This process utilizes the nuclei of the sample's hydrogen atoms to assess their neighboring atoms, revealing the sample's molecular structure (34). Subsequently, through comparison between the spectra of the GelNOR sample and the gelatin used for the synthesis, the DOF can be calculated. This method was not utilized, as the required device was not available in the laboratory.

6.1.3 Hydrogel casting

The GelNOR material was tested by casted discs of approximately 4 mm in diameter and 2 mm in height in a silicone mold in the UV oven, in order to quickly see the possibility of polymerization. In this report, the PI used is LAP[Figure 5A], as it is highly soluble in water (25). We expected the formation of solid, yet flexible Hydrogel discs with a high degree of polymerization. Approximately half of the synthesized GelNOR batches resulted in soft, instable discs. It was plausible that there was a remaining excess of carbic anhydride which inhibits the polymerization reaction of the material with the thiolated crosslinkers. The inhibition mechanism is the same as the crosslinking mechanism, namely the hydrothiolation of the C=C bond of the carbic anhydride, resulting in the excess carbic anhydride competing with the GelNORs functional groups for the crosslinkers thiol groups. Due to this, an additional dialysis step was performed with the GelNOR material to purify it from the excess carbic anhydride. Hereinafter, the test printing was performed again. Illustrated in the GelNOR discs before the additional dialysis step on the left, and the discs, made with two times dialyzed

GelNOR, on the right [Figure 12]. The three spheres on the left showed a low stability and a high content of fluid material on the sides, whereas the four spheres on the right appeared to be stronger and no fluid material was present. We interpret this as a confirmation of our theory, that the presence of excess carbic anhydride inhibits the crosslinking mechanism. A modification of the synthesis protocol might be beneficial. This can be done by prolonging the default time of the dialysis or performing this step at room temperature or up to 40°C. However, dialyzing the material at higher temperatures might also increase the risk of microbial infections (35). Another possible adjustment for the synthesis protocol might be the sequential addition of carbic anhydride and pH adjustment according to Rizzo et al., as it results in a 20-fold reduced amount of required reagent and drastically reduces the reaction time (25). This was not done in this report, since the experiments were carried out before the publication of results by Rizzo et al.

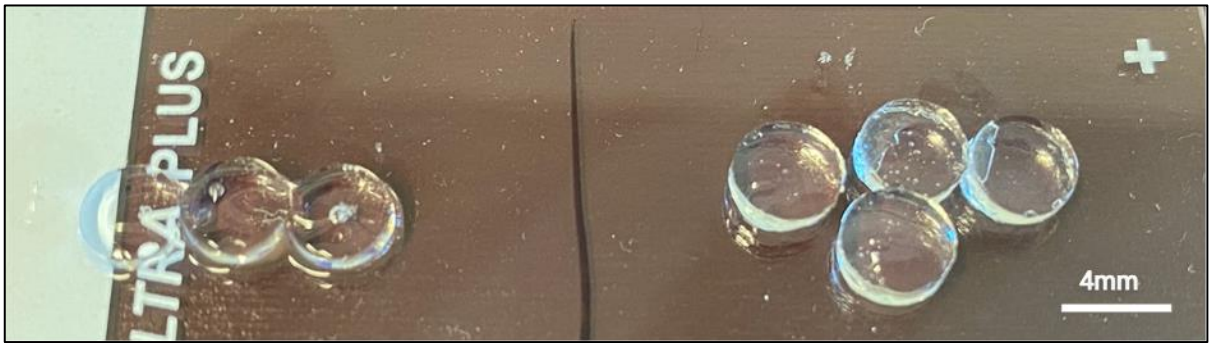

Figure 12: 6.1.3 Hydrogel casting – *Comparison of the GelNOR discs before (left) and after the second dialysis (right). The hydrogels were casted in with a GelNOR concentration of 10% w/v, containing 0.05% w/v LAP and 10mM DTT in an UV-oven for 10 minutes (λ = 365 nm).*

6.2 Optimization of the printing conditions

Following the synthesis and the analysis of the GelNOR, the conditions for the volumetric printing process of GelNOR were assessed. The purpose of these experiments was to find suitable volumetric printing conditions, under which the GelNOR can be printed in an acceptable resolution to print complex structures with small features. The channel in the printed constructs resembles a (blood) vessel and has a diameter of 1.5 mm [Figure 13].

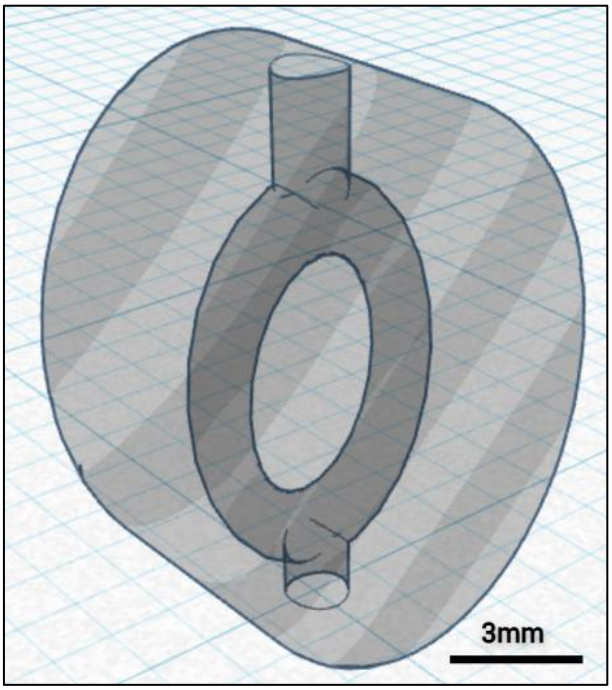

Figure 13: 6.2 Optimization of the printing conditions – *Illustration of the structure to optimize the printing conditions of GelNOR. The oval shaped construct shows a hollow channel, which splits in two circular tubes and merges again, forming an outlet. The channel has a diameter of 1.5 mm and resembles a blood vessel.*

The printing process in this experiment and the underlying chemical reaction has several possible points of adjustment. One of these is DTT, which functions as a crosslinker between two norbornene groups in the hydrogel, thus has influence on the stiffness of the crosslinked construct. The concentration of crosslinker can determine the stiffness of the GelNOR constructs, whereby a higher crosslinker concentration results in a stiffer gel, as stated by Rizzo et al. Another determining factor for the hydrogels properties is the used concentration of GelNOR, which was kept constant throughout this experiment (25). ASAP has the function of capturing radicals and is therefore used to specifically slow down the crosslinking reaction. The exposure time [s] and light intensity [mW/cm2] determine the number of radicals produced during the printing process. Hence, the longer the time of exposure and the higher the light intensity, the higher the degree of polymerization. The principle of the volumetric printing process is to reach the degree of polymerization, where the printed object shows the desired structures and a certain stability, but is not over polymerized in unwanted regions (12). The structure can then be washed and subsequently stabilized in a post-curing process, where it is infused with LAP and a crosslinker and crosslinked in a UV-oven. The time of light exposure and light intensity can be summarized by calculating their product, resulting in the light dose, the hydrogel was exposed to [Equation 4].

Equation 4: 6.2 Optimization of the printing conditions – *Formula to calculate the light dose of the volumetric printing*

$$Exposure\ time\ [s] * Light\ intensity\ [\frac{\mathrm{mW}}{cm^2}] = Light\ dose\ [\frac{\mathrm{mJ}}{cm^2}]$$

This experiment was carried out by printing one hydrogel after the other and adjusting the printing conditions and hydrogel compositions based on the results of the previous. Gel 1 (light dose 696 mJ/cm^2) was not roundly shaped and no channels were inside the construct [Figure 14]. Furthermore, the gel was very stiff. It is plausible, that the gel was over polymerized and the light dose should be lowered or ASAP should be used. Gel 2, being printed without ASAP, but a lower light dose of 448 mJ/cm^2 had the intended round outer shape, but no channels were present in the hydrogel. This is interpreted as an overly crosslinked gel and the light dose was lowered for the following gel to 442 mJ/cm^2. Gel 3 had a round shape, but not uniformly with no sharp edges, what is interpreted as underly crosslinked hydrogel. Additionally, no channels were inside the hydrogel. Therefore, the consecutive gel was printed with a higher light dose of 448 mJ/cm^2, but also containing 0.01% w/v ASAP. Gel 4 dissolved in the printing vial during the washing process with warm PBS. This suggests a weak crosslinking and the printing conditions for gel 5 were adjusted by increasing the light dose to 474 mJ/cm^2. Gel 5 was not shaped uniformly and showed no channels. It is likely, that the concentration of ASAP was too high and was therefore lowered its concentration to a tenth (0.001% w/v). This resulted in gel 6 having a uniformly round shape without channels being present. This is interpreted as a slight over-crosslinking and the amount of ASAP was therefore increased to 0.005% w/v for the next hydrogel. Despite using more ASAP to inhibit the crosslinking reaction, gel 7 showed a higher degree of over-crosslinking. This was manifested in the absence of channels in the gel and the construct being bigger than the used printing template. To overcome this, gel 8 was printed with the same ASAP concentration, but with a lower light dose of 442 mJ/cm^2. Gel 8 dissolved in the printing vial during the washing process with warm PBS, what is interpreted as a low degree of crosslinking.

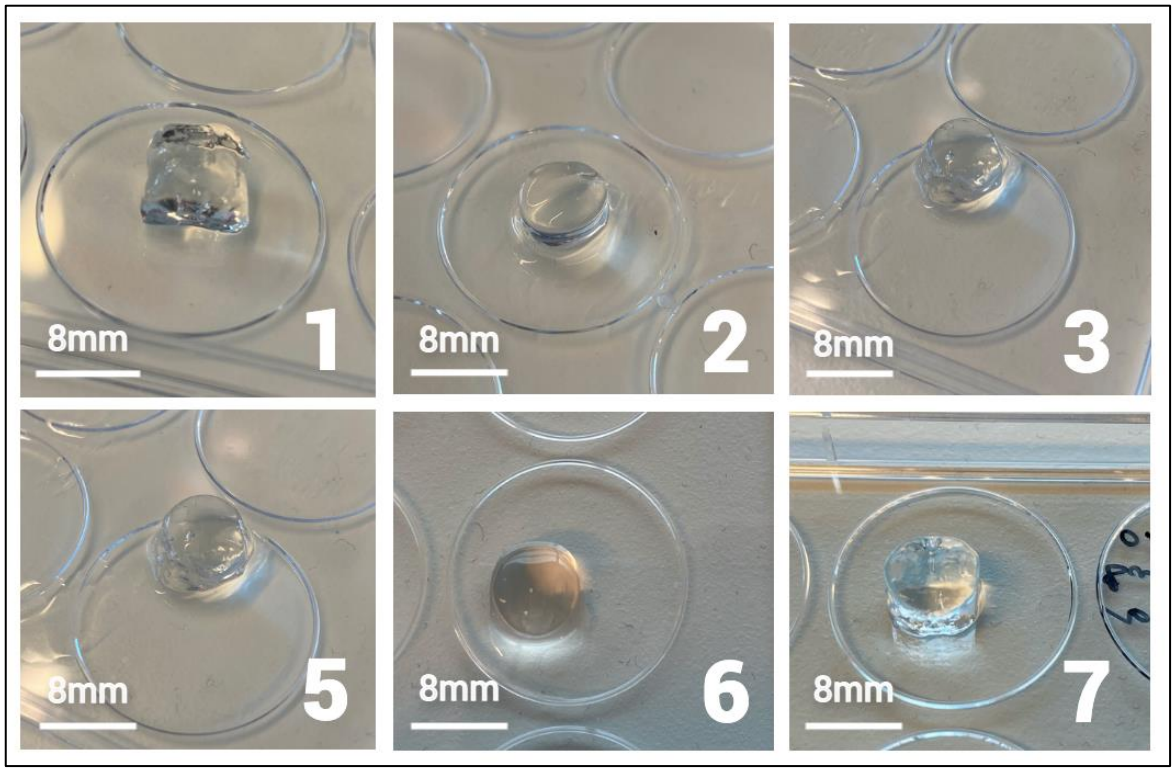

Figure 14: 6.2 Optimization of the printing conditions – *Pictures of gel 1,2,3,5,6, and 7. All gels were printed in a volumetric printer with a GelNOR concentration of 10% w/v and 0.05% w/v LAP. The varying factors between the gels were the concentration of DTT and ASAP in the hydrogel and the light dose during the printing process.*

Gel 9, printed with a lower concentration of ASAP compared to the previous gel (0.001% w/v), had a round outer shape and the channel inlet started forming [Figure 15]. The gel seemed to be over crosslinked and the ASAP concentration and the light dose was increased for the next gel to 0.005% w/v ASAP and a light dose of 458 mJ/cm^2. Gel 10 had a uniformly round shape, but also no channels present. To circumvent this over crosslinking, the light dose and the ASAP concentration was reduced (0.001% w/v ASAP and 442 mJ/cm^2). Additionally, the concentration of DTT in the hydrogel was reduced from 8mM to 6mM. This resulted in gel 11 dissolving in the printing vial during the washing process with warm PBS. Accordingly, the light dose was increased to 455 mJ/cm^2 for the following printing process and there was no ASAP added to the hydrogel. Gel 12 partially dissolved during the washing process in the printing vial with warm PBS, hence showed an irregular outer shape. Despite the outer shape not being uniformly, gel 12 had channels within the hydrogel which could be flooded with air. This can be seen as an improvement over the previous gels. To prevent the dissolving of the outer parts of the gel, the light dose for the following print was increased to 460 mJ/cm^2. Gel 13 had a round outer shape, but no channels present, what is interpreted this as an over crosslinking of the gel.

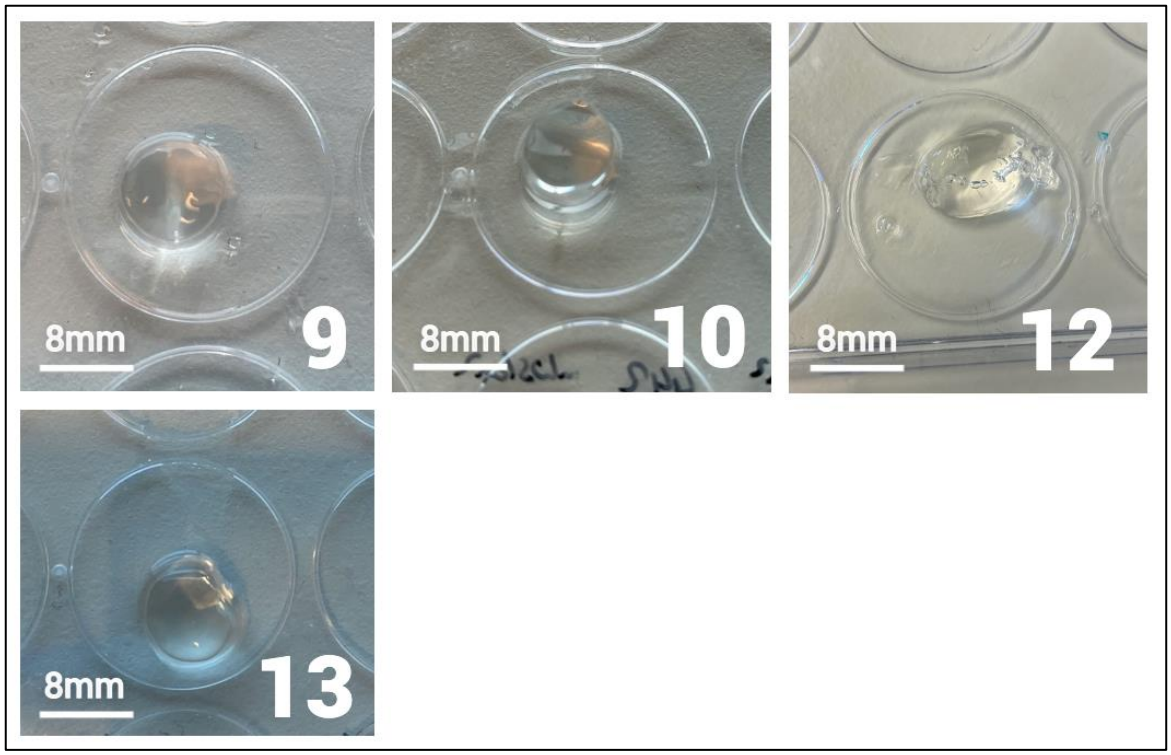

Figure 15: 6.2 Optimization of the printing conditions – *Pictures of gel 9,10,12, and 13. All gels were printed in a volumetric printer with a GelNOR concentration of 10% w/v and 0.05% w/v LAP. The varying factors between the gels were the concentration of DTT and ASAP in the hydrogel and the light dose during the printing process.*

These experiments were stopped due to high batch to batch variations of the used GelNOR. Comparing these results with Rizzo et al. [Figure 7] it is obvious, that the printing times in the experiments by Rizzo et al. were significantly shorter. The printing time in this report ranged from 1.5 – 2 minutes, whereas Rizzo et al. printed GelNOR constructs within 10-11 seconds. This is also the case for the used light doses, used during the printing process, being 80-90 mJ/cm^2 used by Rizzo et al. and a minimum of 442 mJ/cm^2 in this report. Furthermore, Rizzo et al. were able to print in a higher resolution of approximately 200 μm. This can be explained by the fact, that Rizzo et al. used a different crosslinker molecule, namely PEG4SH [Figure 8]. With PEG4SH having four thiol groups, the crosslinking is significantly stronger and faster, compared to the crosslinking with DTT as a crosslinker, only having two thiol groups. This is due to the fact, that one crosslinker molecule of PEG4SH crosslinks 4 norbornene groups of GelNOR, instead of only 2 for DTT. Further, Rizzo et al. had a norbornene to thiol ratio of 1:1, meaning the concentration of thiol groups within the bioink matched the norbornene group's concentration, resulting in a rapid and strong crosslinking (25). However, the experiments in this report were deliberately performed with a lower degree of norbornene saturation, as it was aimed to spare functional norbornene groups within the hydrogel for further modification. This experiment could have been improved by incubating the crosslinked constructs in 37°C PBS on an orbital shaker for 24 h to thoroughly remove all the un-crosslinked material.

6.3 Grafting of biological molecules into GelNOR

The purpose of the grafting experiments is to find suitable conditions to graft biological molecules into an already crosslinked construct of GelNOR in a spatially controlled way. One molecule of DTT reacts with two norbornene groups during the crosslinking process. Therefore, the DTT concentration has to be 35% of the concentration of norbornene groups in the hydrogel in order to reach a saturation of 70%. The GelNOR batch, used for the production of hydrogel cylinders in the following experiments, was used in a concentration of 5% w/v. This corresponds with a norbornene group concentration of 12mM. Accordingly, the concentration of DTT for the crosslinking was 4.2mM to reach a saturation of norbornene groups of approximately 70%.

With ascorbate being one of the most effective water-soluble antioxidants (radical scavenger), the addition of ASAP to the infusion mix might not be beneficial for the modularity of the grafting process (36). Therefore, TEMPO was used to modulate the grafting process, as it mediates the concentration of radicals by a reversible termination step with its low bond dissociation energy (37).

6.3.1 Grafting feasibility

To prove the possibility of grafting biological molecules onto GelNOR, we chose the modified BSA as a grafting material. We expected the BSA to be suitable, because it has an odd number of cysteine groups, hence at least one cysteine rest is not involved in as disulfide bridge (38).

Some of the gels were damaged during the cutting process, resulting in amorphous slices. The exposure time of the camera was adjusted automatically by the camera. Hence, the colors and therefore the intensity of the gels differ. The pictures were taken of the part of the cylinder, where the printing was performed and the grafting was expected. The sides of each cylinder showed a higher intensity. This is interpreted as being a refraction of the light, the cylinders were exposed with. The cylinders showed a high background signal. It is plausible, that the washing process after the grafting is not efficient due to the large molecule weight of the BSA (approximately 66.5 kDa). The following images [Figure 16 & Figure 17] were captured with a normal camera through the eyepiece of the microscope. Therefore, the gels differ in color intensity, as the camera's shutter speed was set automatically.

Cylinder 1, just being infused with BSA without LAP and TEMPO, underwent no printing process. The color of the gel was transparent by the eye, but changed to homogeneously orange under the exposure of green light under the microscope and bubbles were inside the Gel [Figure 16]. The color homogeneity is interpreted as BSA residues without a specific binding to the material, but merely due to adsorption to the hydrogel. Therefore, the following gels were expected to have a similar background color. An additional washing step could reduce the background signal.

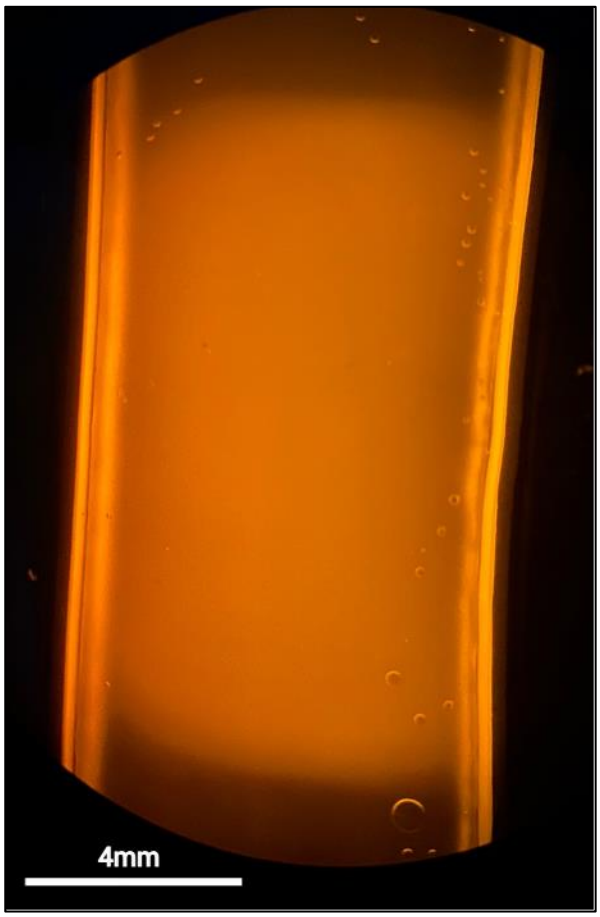

Figure 16: 6.3.1 Grafting feasibility – *Picture of cylinder 1, a reference infused with no LAP or TEMPO and no grafting. The hydrogel cylinder had a concentration of 5% w/v GelNOR and were crosslinked with 4.2mM DTT and 0.05% w/v LAP in an UV-Oven for 10 minutes. The fluorescent dye in this cylinder is the modified BSA.*

Cylinder 2 was deformed during the cutting process [Figure 17]. Nevertheless, it showed 3 horizontal bands, where the discs were printed with the highest light doses. The bands intensity was the highest in the cylinders center. Cylinder 3 was infused with twice the amount of LAP and showed 5 clear bands, of which the top 3 showed a higher intensity in their center. The bottom 3 bands were not entirely straight. The intensity of the bands seemed to increase from the top band to the second and to constantly decrease from there on in the lower bands. Cylinder 4, again infused with only 0.5% w/v LAP but also 0.006% w/v TEMPO, showed 4 curved bands with an increasing intensity from top to bottom. The intensity of the bands in cylinder 4 was lower compared to the cylinders without TEMPO. Cylinder 5 was infused with the same amount of TEMPO as cylinder 4, but a concentration of LAP of 1% w/v. This resulted in 5 distinct bands, decreasing in intensity from top to bottom. The top 3 bands were ruptured at the left third of the band and bent downwards. These bands also showed a higher intensity in their center. Compared to cylinder 4, cylinder 5 showed bands of higher intensity, with the only difference in the infusion conditions being a higher concentration of LAP. Cylinder 6 was deformed during the cutting process and shows no bands. Cylinder 6 was infused with the highest TEMPO concentration (0.0012% w/v) and the lowest LAP concentration (0.5% w/v).

Cylinder 7, infused with the same TEMPO concentration as cylinder 6 but a higher LAP concentration of 1% w/v, was also deformed during the cutting process and showed 2 full bands throughout the gel. Below the 2 bands is a grafted structure in the center of the gel.

The bands are interpreted as fluorescent activity of the modified BSA, being grafted into the GelNOR cylinders. Thereby, the principle of grafting biological molecules into GelNOR was proven to be feasible. We expected the grafted areas to be smaller, since the printed discs had a smaller diameter than the cylinder. This was probably due to an overexposure of light, leading to an unspecific grafting process. The different intensities of the bands within the same cylinders make it seem plausible, that the amount of grafted material is depending on the light dose, as it is the only varying factor between the printed discs within the same cylinder. Another striking fact is the higher intensity of bands in cylinders with higher LAP concentrations, but the same amount of TEMPO (2&3, 4&5 and 6&7). It can therefore be concluded, that the concentration of LAP in the infusion solution has an impact on the amount of dye being grafted into the hydrogel. Another phenomenon spectated is the decreasing intensity of bands, that corresponds with an increasing amount of TEMPO in the infusion solution. This is likely the inhibiting effect of TEMPO, which captures the LAP radicals and therefore slows down the reaction. Even though the grafting of molecules into hydrogels has been achieved by research groups, such as by Broguiere et al., who used two-photon patterning to engraft fluorescein modified biomolecules into matrices of hydrogels based on fibrin, collagen, hyaluronic acid and matrigel, this has never been done with GelNOR in a volumetric printing process in a spatially controlled way (39). This is a breakthrough in VBP, as the process combines the fast process pace of the volumetric printing with the high versatility of GelNOR as a printing material. A possible way to improve this experiment would be a faster freezing process in liquid nitrogen, as it was performed for the following experiments. The faster freezing process minimized the occurring of bubbles within the hydrogels. Another crucial step in the cutting process is to dip the blades in PBS to prevent the gel slice from sticking to it. This would have prevented the slices from deforming during the cutting process.

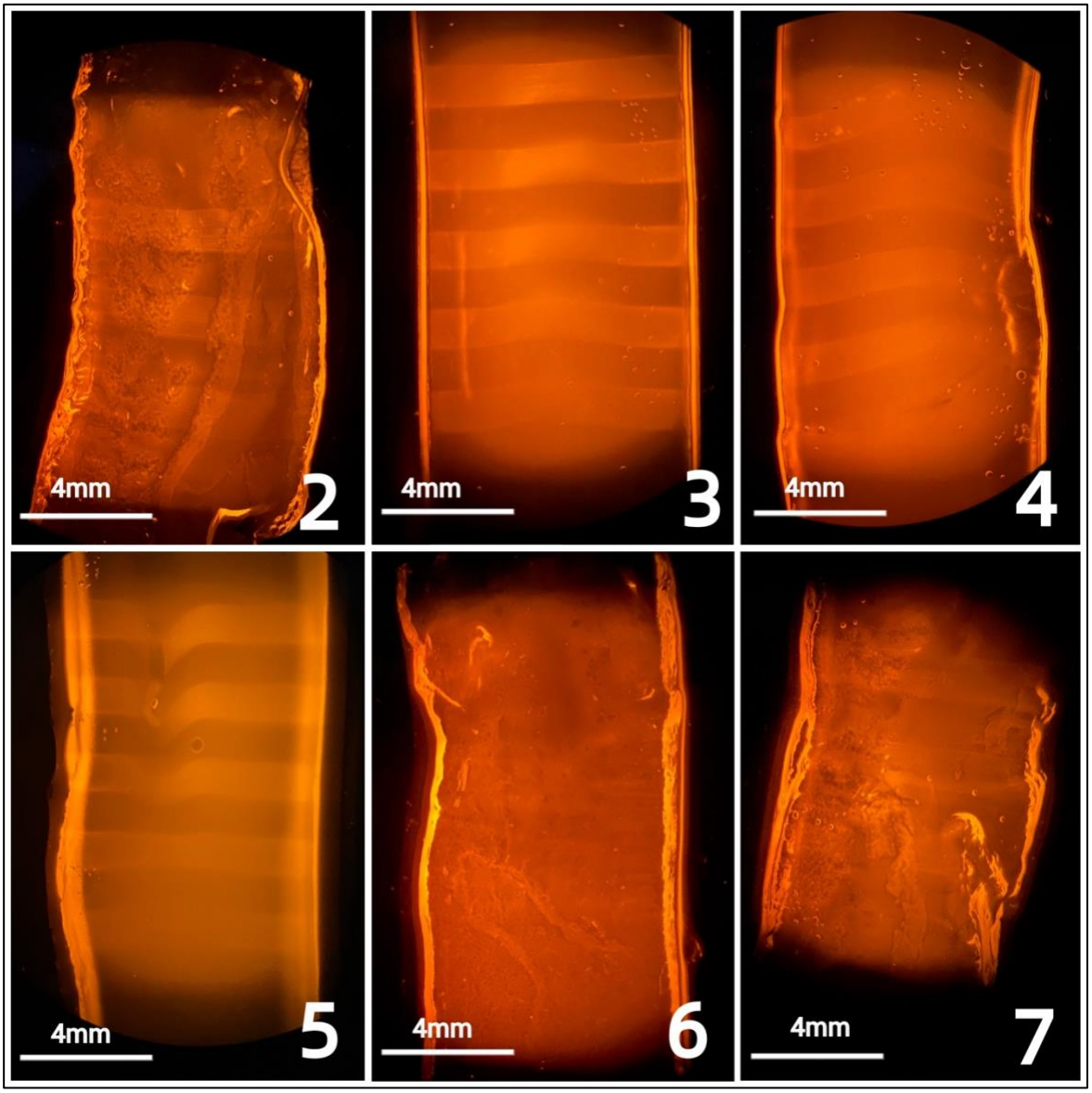

Figure 17: 6.3.1 Grafting feasibility – *Picture of cylinder 2 to 7. The hydrogel cylinder had a concentration of 5% w/v GelNOR and were crosslinked with 4.2mM DTT and 0.05% w/v LAP in an UV-Oven for 10 minutes. The fluorescent dye in this cylinder is the modified BSA. The varying conditions between the cylinders were concentration of LAP and TEMPO, the cylinders were infused with. The light dose, used to graft the discs, decreases with each band within the gel.*

6.3.2 Grafting optimization

After proving the possibility of grafting and finding mechanisms to influence the process, a follow up experiment was designed to find suitable infusing and printing conditions to graft with a resolution. The grafting material for this and the following experiments was PEG-Cy3 [Figure 18], as it is a smaller molecule (5kDa) than the BSA (66.5kDa) and therefore faster to infuse the hydrogel with and to wash it out of it.

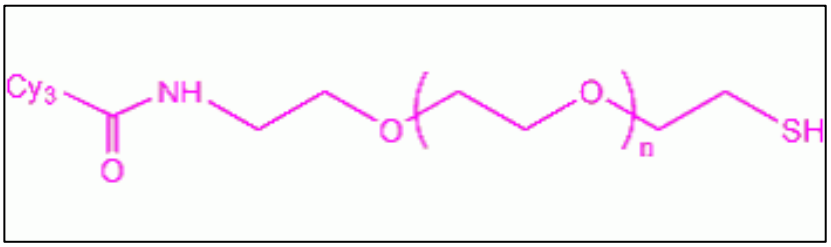

Figure 18: 6.3.2 Grafting optimization – *Schematic of the used grafting material PEG-Cy3 (40).*

The thiol group, coated to the PEG was expected to serve the same function as the cysteine group in the albumin by building a thiol bond with the norbornene groups within the GelNOR. The cylinders' images [Figure 19, Figure 20, Figure 21] consist of squares, which is due to the raster-imaging method of the microscope. The printed discs were located in the middle or the right/left third of the cylinder and were decreasing in intensity from the top to the bottom (see the materials and methods section). The varying localization of the discs can be explained by the placement of the cylinders within the printing vial, whereby a non-concentrical placement resulted in the discs not being grafted in the middle of the cylinder. Placing the cylinder in the center more thoroughly can prevent this phenomenon. Each disc had bands on each side and their intensity is also decreasing from top to bottom. The presence of discs and bands indicates a successful grafting process with PEG-Cy3. The distinctness between the discs and their respective bands provides evidence of a controlled grafting process with minor occurrence of unspecific grafting. The high contrast between the background signal and the printed discs confirms the theory of PEG-Cy3 being easier/faster to wash out of the hydrogel. A post acquisition processing of the pictures by the microscope's software would have removed the squares by merging the raster-imaged pictures, hence improved the quality of the pictures and the data, that was derived from it.

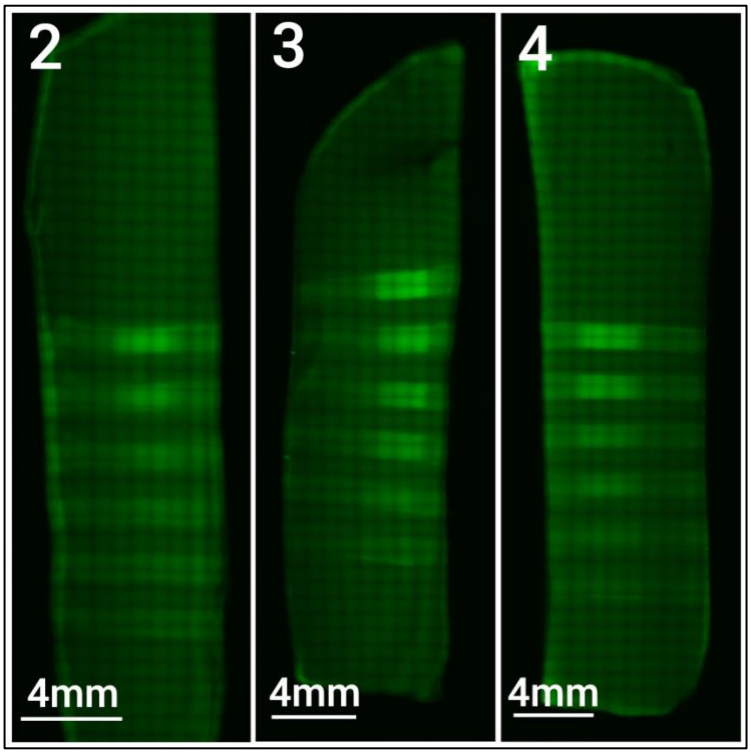

Figure 19: 6.3.2 Grafting optimization – *Collage of the cylinders 2-4 to assess optimal grafting conditions. The hydrogel cylinder had a concentration of 5% w/v GelNOR and were crosslinked with 4.2mM DTT and 0.05% w/v LAP in an UV-Oven for 10 minutes. PEG-Cy3 was used as a fluorescent dye. The varying conditions between the cylinders were concentration of LAP and TEMPO, the cylinders were infused with. The light dose, used to graft the discs, decreases with each band within the gel.*

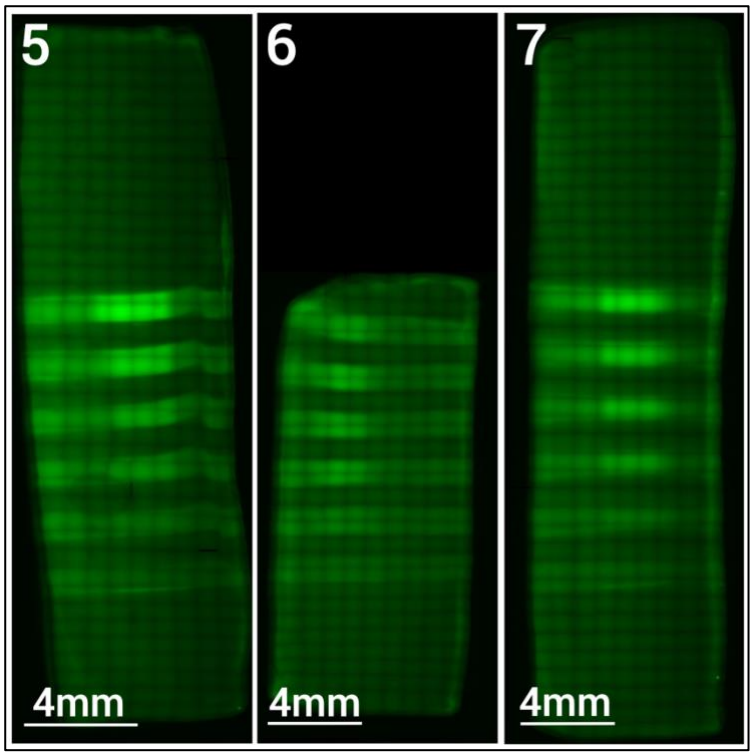

Figure 20: 6.3.2 Grafting optimization – *Collage of the cylinders 5-7 to assess optimal grafting conditions. The hydrogel cylinder had a concentration of 5% w/v GelNOR and were crosslinked with 4.2mM DTT and 0.05% w/v LAP in an UV-Oven for 10 minutes. PEG-Cy3 was used as a fluorescent dye. The varying conditions between the cylinders were concentration*

of LAP and TEMPO, the cylinders were infused with. The light dose, used to graft the discs, decreases with each band within the gel.

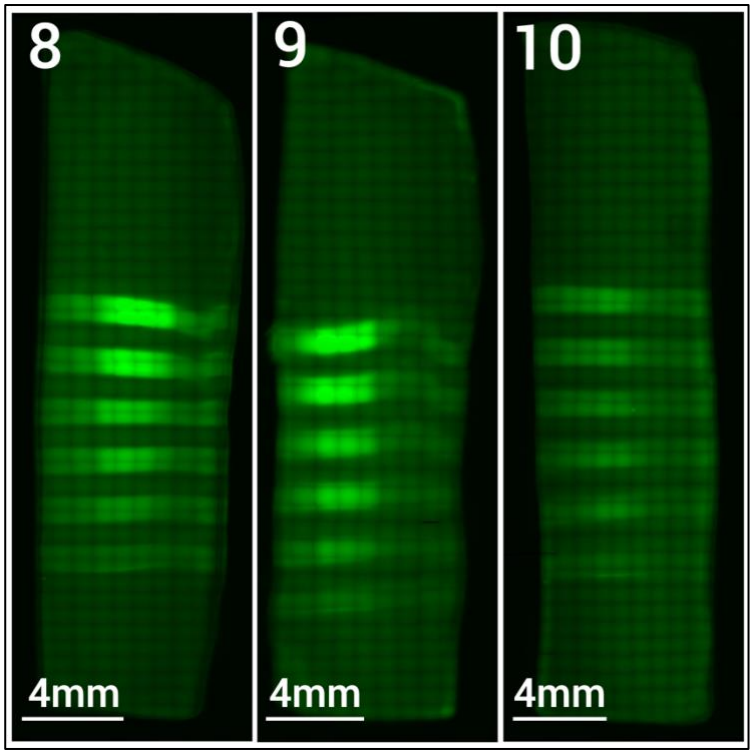

Figure 21: 6.3.2 Grafting optimization – *Collage of the cylinders 8-10 to assess optimal grafting conditions. The hydrogel cylinder had a concentration of 5% w/v GelNOR and were crosslinked with 4.2mM DTT and 0.05% w/v LAP in an UV-Oven for 10 minutes. PEG-Cy3 was used as a fluorescent dye. The varying conditions between the cylinders were concentration of LAP and TEMPO, the cylinders were infused with. The light dose, used to graft the discs, decreases with each band within the gel.*

To further analyze the grafted hydrogels, the acquired pictures of each hydrogel were analyzed with ImageJ in order to quantify the grafting resolution. By analyzing the average intensity of the printed discs, the average intensity next to the discs and the average intensity of the background of the cross-section, 3 different ratios were calculated. The first ratio (Ratio1) is the ratio between the average disc intensity and the average intensity of the section next to the respective disc [Equation 5].

Equation 5: 6.3.2 Grafting optimization – *Formula to calculate Ratio1*

$$Ratio1 = \frac{Average\ intensity\ disc}{Average\ intensity\ sides}$$

The second ratio (Ratio2) is the ratio between the section next to the analyzed disc and the average intensity of the background [Equation 6].

Equation 6: 6.3.2 Grafting optimization – *Formula to calculate Ratio2*

$$Ratio2 = \frac{Average\ intensity\ sides}{Average\ intensity\ background}$$

Ratio1 serves the purpose of creating a sharp distinction between the disc and the unspecific grafting to its sides. Therefore, a cutoff value with a lower limit was chosen, since the difference of the values is desired to be as big as possible. The limit for Ratio1 in this experiment is >2.300 and was generated by slowly decreasing the cutoff value, until several valued were withing the cutoff value. Ratio2 was calculated to minimize the difference between the unspecific grafting on the sides of the discs and the background, hence minimizing the unspecific grafting. Therefore, a cutoff value with an upper limit was selected, since the difference of the values should be as low as possible. The limit for Ratio2 in this experiment is <1.500. Analogue to Ratio1, this cutoff value was obtained by gradually decreasing the value, until values were above the cutoff limit.

To further improve the selection process, a third ratio (Ratio3) was calculated by dividing Ratio1 by Ratio2. The formula can be seen in Equation 7.

Equation 7: 6.3.2 Grafting optimization – *Formula to calculate Ratio3*

$$Ratio3 = \frac{Ratio1}{Ratio2}$$

As it is desirable for Ratio1 to be as big and Ratio2 to be as small as possible, a cutoff value with a lower limit for Ratio3 was implemented to further improve the analysis. The cutoff value for Ratio3 in this experiment was >1.950 and the value obtained in the same way as for Ratio2.

All discs, which fulfilled the ratio criteria (Disc 1 of gel 3, 5 and 9), were printed with a light dose of 2000 mJ/cm^2[**Table *6***]. This makes it plausible, that the grafting process is slower than the crosslinking of GelNOR or has a higher threshold for the reaction to start, since the crosslinking takes a significantly lower light dose. This is a desirable feature of the grafting process, as a slower mechanism allows for a controlled grafting process with relatively high resolution, considering the fast pace of the crosslinking reaction. Another possible explanation for this phenomenon is, that the PEG-Cy3 needs to be grafted into the GelNOR in higher concentrations to be detected, than the number of crosslinks necessary for a stable crosslinking. This seems plausible, since 70% of the hydrogels norbornene groups were occupied after the crosslinking. The experiment's entire range of LAP concentrations can be found among the valid discs, making it likely, that even though the concentration of LAP plays a role in the grafting, the whole range used in the experiment is suitable. Concentrations of TEMPO at 0.01 w/v% did not seem suitable for grafting with resolution. This is interpreted as TEMPO inhibiting the grafting reaction too much by capturing the LAP radicals. The proportion of LAP and TEMPO also seems to play a significant role in the grafting process. Disc1 of gel 3 had a proportion of 75/1 for LAP to TEMPO and gave significantly lower results for Ratio1 and Ratio2, whereas Disc1 of gel5 and Disc1 of gel9 both had a LAP to TEMPO proportion of 100/1

and 125/1, resulting in significantly higher Ratio1 and Ratio2 values. This suggests that a lower proportion of LAP compared to TEMPO reduces the intensity of the intended disc in comparison to its sides. This was surprising, since the intended use of TEMPO is to reduce the unspecific grafting. Additionally, the lower proportion of LAP to TEMPO seems to lower the difference between the sides of the discs compared to the background signal. This seems logical, since the higher TEMPO concentration in comparison to LAP blocks the general grafting mechanism, whereas the background signal is caused by simple residues of dye and is not affected by the LAP and TEMPO concentration. Considering these insights, the following experiments were carried out with a LAP to TEMPO proportion of >75/1.

The values of all discs for ratio1 give an average value of 1.7964 with a relative standard deviation of 23.5%. Ratio2 has an average value of 1.2584 and a relative standard deviation of 16.8%. The results of Ratio3 average at 1.4447, showing a relative standard deviation of 21.7%. The average values for ratio1 and ratio3 were not within the specified limits, indicating that the average value for the varying parameters remain to be optimized. All three ratios gave a relatively high relative standard deviation. This could be improved by narrowing the range of the varying experimental parameters.

	Disc	LAP [w/v%]	TEMPO [w/v%]	Light dose [mJ/cm²]	Ratio1	Ratio2	Ratio3
Gel2	1	0.6	0.006	2000	2.1991	1.1268	1.9516
Gel2	2	0.6	0.006	1750	1.8667	1.0976	1.7007
Gel2	3	0.6	0.006	1500	1.5070	1.0488	1.4369
Gel2	4	0.6	0.006	1250	1.3287	1.0537	1.2610
Gel2	5	0.6	0.006	1000	1.2677	0.9659	1.3125
Gel2	6	0.6	0.006	750	1.2443	0.8585	1.4493
Gel3	1	0.6	0.008	2000	2.3959	1.1893	2.0145
Gel3	2	0.6	0.008	1750	2.1564	1.1796	1.8280
Gel3	3	0.6	0.008	1500	1.8913	1.1165	1.6940
Gel3	4	0.6	0.008	1250	1.8717	1.0971	1.7060
Gel3	5	0.6	0.008	1000	1.6473	1.0874	1.5149
Gel3	6	0.6	0.008	750	1.5503	0.9175	1.6897
Gel4	1	0.6	0.010	2000	2.2393	1.1196	2.0001
Gel4	2	0.6	0.010	1750	2.0676	1.0622	1.9465
Gel4	3	0.6	0.010	1500	1.7356	0.9952	1.7439
Gel4	4	0.6	0.010	1250	1.7512	0.9809	1.7854
Gel4	5	0.6	0.010	1000	1.4513	0.9330	1.5555
Gel4	6	0.6	0.010	750	1.3631	0.8565	1.5916
Gel5	1	0.8	0.006	2000	2.8597	1.4632	1.9545
Gel5	2	0.8	0.006	1750	2.3564	1.4474	1.6280
Gel5	3	0.8	0.006	1500	1.9960	1.3158	1.5170
Gel5	4	0.8	0.006	1250	1.6932	1.3895	1.2186
Gel5	5	0.8	0.006	1000	1.6045	1.1579	1.3857
Gel5	6	0.8	0.006	750	1.3632	1.0579	1.2886
Gel6	1	0.8	0.008	2000	1.6537	1.4150	1.1687
Gel6	2	0.8	0.008	1750	1.6318	1.4800	1.1025
Gel6	3	0.8	0.008	1500	1.5552	1.4500	1.0725
Gel6	4	0.8	0.008	1250	1.5368	1.4250	1.0785
Gel6	5	0.8	0.008	1000	1.4478	1.3400	1.0804
Gel6	6	0.8	0.008	750	1.2958	1.2000	1.0799
Gel7	1	0.8	0.010	2000	2.2825	1.6042	1.4228
Gel7	2	0.8	0.010	1750	2.1927	1.4323	1.5309
Gel7	3	0.8	0.010	1500	2.0769	1.3542	1.5337
Gel7	4	0.8	0.010	1250	1.8871	1.2917	1.4610
Gel7	5	0.8	0.010	1000	1.5682	1.1458	1.3686
Gel7	6	0.8	0.010	750	1.3858	1.0260	1.3506
Gel8	1	1.0	0.006	2000	2.2432	1.7264	1.2993

Gel8	2	1.0	0.006	1750	2.2397	1.7123	1.3080
Gel8	3	1.0	0.006	1500	1.8716	1.5425	1.2134
Gel8	4	1.0	0.006	1250	1.7810	1.4434	1.2339
Gel8	5	1.0	0.006	1000	1.4657	1.3066	1.1218
Gel8	6	1.0	0.006	750	1.1434	1.1840	0.9658
Gel9	1	1.0	0.008	2000	2.8253	1.4106	2.0029
Gel9	2	1.0	0.008	1750	2.7254	1.4251	1.9124
Gel9	3	1.0	0.008	1500	2.3718	1.3382	1.7725
Gel9	4	1.0	0.008	1250	2.3700	1.3188	1.7970
Gel9	5	1.0	0.008	1000	1.8452	1.2174	1.5157
Gel9	6	1.0	0.008	750	1.4279	1.1063	1.2908
Gel10	1	1.0	0.010	2000	1.6007	1.5421	1.0380
Gel10	2	1.0	0.010	1750	1.4698	1.4789	0.9938
Gel10	3	1.0	0.010	1500	1.4926	1.4211	1.0503
Gel10	4	1.0	0.010	1250	1.5204	1.4158	1.0739
Gel10	5	1.0	0.010	1000	1.4886	1.3895	1.0714
Gel10	6	1.0	0.010	750	1.2033	1.2947	0.9293

Table 6: 6.3.2 Grafting optimization – *Calculated values for ratio1-3 and the respective grafting conditions of the discs for the disc grafting experiment to optimize the grafting conditions. The hydrogel cylinders had a concentration of 5% w/v GelNOR and were crosslinked with 4.2mM DTT and 0.05% w/v LAP in an UV-Oven for 10 minutes. PEG-Cy3 was used as a fluorescent dye. The varying conditions between the cylinders were concentration of LAP and TEMPO, the cylinders were infused with and the light dose, used to graft the discs.*

For a more detailed analysis of the values above, the average value for Ratio1-3 for the discs within the same gel was calculated, as the variation of discs (light dose) within each gel was the same and can therefore be neglected [Table 7]. The average values for ratio1 of each gel do not seem to correspond with the amount of LAP the gel has been infused with. This can be explained with the fact, that regardless of the concentration of LAP, the grafting reaction is triggered after passing the light dose threshold. This is the case for the intended grafting area, as well as in the unintended, especially in the horizontal plane, since discs were projected into the hydrogel from a horizontal plane. A possible cause for this phenomenon could be a light scattering effect of the PEG-Cy3. If this is the case, a series of experiments, analogue to experiments carried out by Bernal et al., who added substances to their bioink in order to adjust the bioinks refractive index to the scattering components within it, could solve this issue (16). The intended use of TEMPO is to provide a certain threshold, in order to prevent the unspecific grafting process, but allow the grafting process in intended areas, thereby increasing the grafting resolution. Why this is not the case remains to be determined. A subsequent experiment with a different concentration range of TEMPO might be beneficial to find a suitable concentration. Additionally, the substitution of TEMPO in the bioink with a fainter photo inhibitor could allow for a higher degree of modification and thereby a higher resolution of the grafting process. However, the values of Ratio2 show a strong correlation with the concentration of LAP in the infusion solution. This seems plausible, as a higher amount of LAP radicals also promotes the unspecific grafting next to the intended discs, but not the background signal. Ratio3 does not seemingly correspond with the concentration within the infusion mix. This can be explained with the fact, that it is calculated by the division of Ratio1 and Ratio2. As Ratio1 does not correspond with the infusion conditions, it mathematically logical, that Ratio3 does not correspond as well.

Gel	LAP [w/v%]	TEMPO [w/v%]	Average Ratio1	Average Ratio2	Average Ratio3
2	0.6	0.006	1.5689	1.0252	1.5187
3	0.6	0.008	1.9188	1.0979	1.7412
4	0.6	0.010	1.7680	0.9912	1.7705
5	0.8	0.006	1.9788	1.3053	1.4987
6	0.8	0.008	1.5202	1.3850	1.0971
7	0.8	0.010	1.8989	1.3090	1.4446
8	1.0	0.006	1.7908	1.4859	1.1904
9	1.0	0.008	2.2609	1.3027	1.7152
10	1.0	0.010	1.4626	1.4237	1.0261

Table 7: 6.3.2 Grafting optimization – *Average values of ratio1-3 for each gel and the corresponding grafting conditions for the disc grafting experiment to optimize the grafting conditions.*

The following graphs give an illustration of ratio1-3 of each disc in each gel [Figure 22]. The blue bars correspond with ratio1 for each disc, the orange bar with ratio2 and the grey bar with ratio3. The x-axis of each graph shows the various discs of each gel and the values for each ratio is plotted on the y-axis. Ratio1 shows a high variation with the light dose, which was used to graft the discs. Throughout every gel, the value for ratio1 decreases with the light doses being lowered. This makes the theory plausible, that the grafting reaction has a higher threshold than the crosslinking reaction, since a higher light dose has a higher effect on the specific grafting than it has on the unspecific. In consequence, this means that the grafting process can be tuned by the light dose, giving control over the process and its resolution. Ratio2 gives mostly stable results throughout each gel and only slightly decreases with lower light doses for each disc. This means, that neither the background signal, nor the signal of the unspecific grafting areas is depending on the light dose, used for the grafting process. This makes the theory plausible, that the background signal is merely depending on the washing step after the grafting process. This ultimately means, that by adding an additional washing step to the experiment, the background signal would be reduced, resulting in an increase in the values for Ratio2. This would cause the necessity of setting a new cutoff value for Ratio2 and ultimately Ratio3. With Ratio3 being calculated with Ratio1 and Ratio2, it seems logical for Ratio3 to be seemingly half as much depending on the light dose as ratio1. As it is desirable for the values of Ratio3 to be as high as possible, conditions resulting in a high value for Ratio1 should be selected, what can be achieved by using a high light dose for the grafting. Similarly, infusion conditions causing a low value for Ratio2 are to be aimed at. This is possible by using lower concentrations of LAP.

A further improvement of this experiment could be achieved by adjusting the formula of Ratio2 by dividing the intensity of the background signal by the intensity of the unspecific grafting on the side of the discs. The desired value for this new Ratio2 would be 1, as this would be the result for Ratio2 if the intensities would be the same. That would mean, that there was no occurrence of unspecific grafting, which is highly desirable. This was not done in this report, as the experiments and their evaluation were performed after this finding.

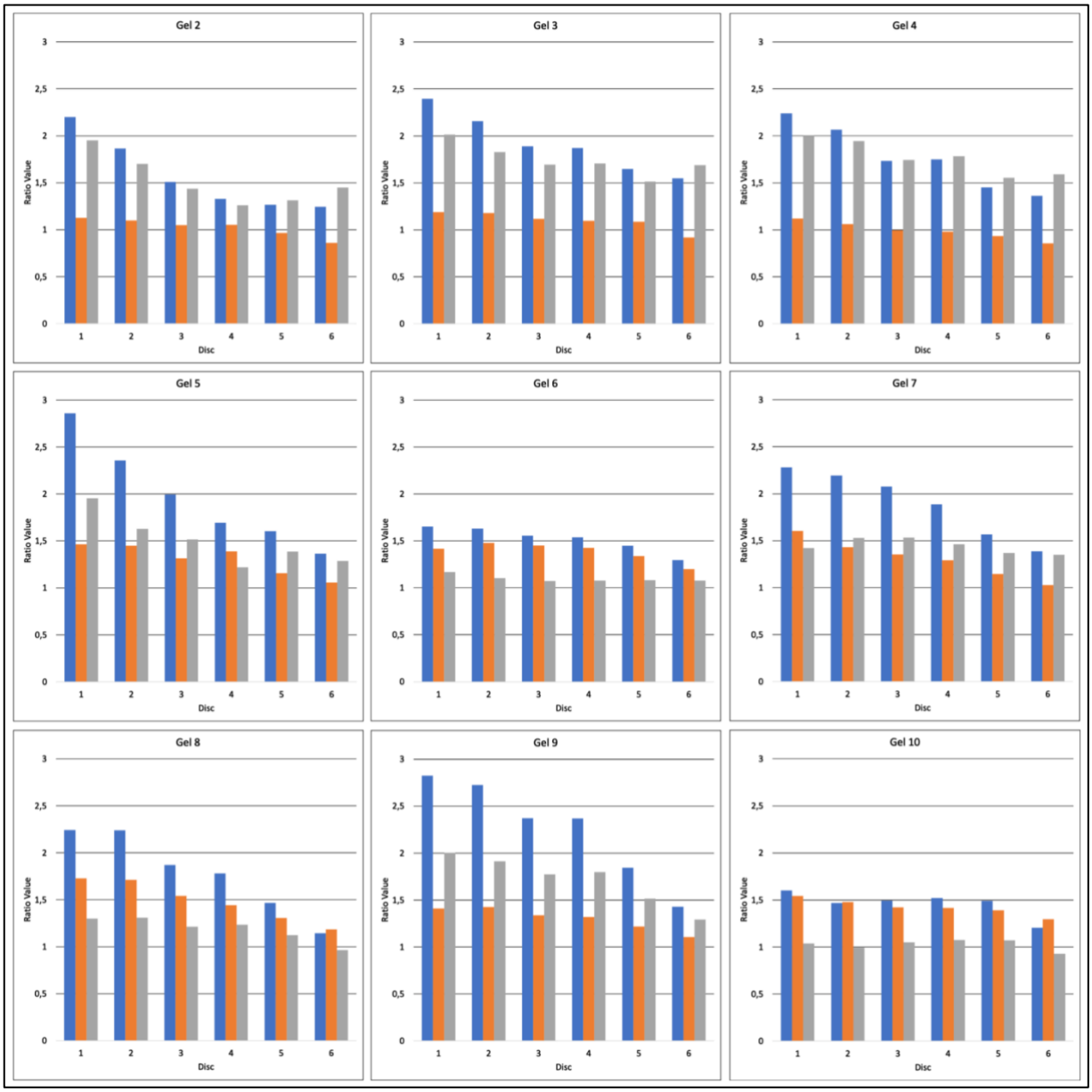

Figure 22: 6.3.2 Grafting optimization – *Graphical illustration of the data retrieved from picture analysis of the disc grafting experiment. The blue bars depict ratio1 for each gel. Analogically, ratio2 is portrayed by the orange bar and ratio3 by the grey. The hydrogel cylinder had a concentration of 5% w/v GelNOR and were crosslinked with 4.2mM DTT and 0.05% w/v LAP in an UV-Oven for 10 minutes. PEG-Cy3 was used as a fluorescent dye. The varying conditions between the cylinders were concentration of LAP and TEMPO, the cylinders were infused with and the light dose, used to graft the discs.*

In the subsequent experiment, a two-dimensional fractal was printed under several conditions to refine the grafting conditions, based on the results of the previous experiments. We chose the fractal structure as a grafting template, as it is significantly more complex than the previously printed discs. The fractal had a width of 7mm, a thickness of 1mm and a total height of 17mm [Figure 23].

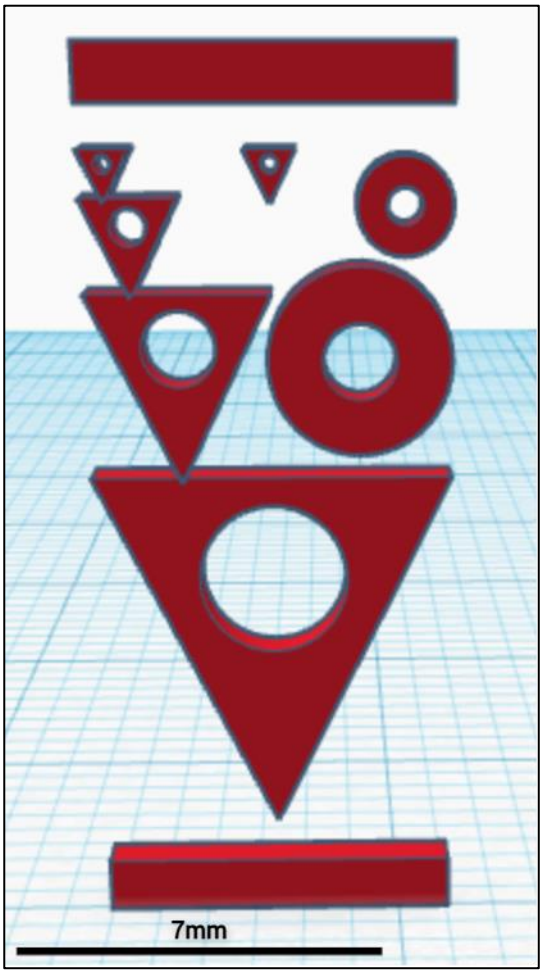

Figure 23: 6.3.2 Grafting optimization – *Template of the two-dimensional fractal, used to optimize the grafting conditions. The fractals thickness is 1mm, its width 7mm and the total height is 17mm. PEG-Cy3 was used as a fluorescent dye and the fractals grafted with a light dose of 2000 mJ/cm².*

A two-dimensional structure was the logical step to further assess the grafting resolution, since it was possible to analyze in the laboratory, as the facilities were not equipped with a possibility to analyze a three dimensionally grafted structure. In this experiment was crucial to find the correct plane within the cylinder to cut the central cross-section. This is due to the fact, that the two-dimensional fractal was grafted into a three-dimensional hydrogel cylinder and to detect the grafted area it is vital to cut out the correct plane of the cylinder. In order to do so, the copy of the fractal structure was printed above the initial one to possibly see the grafted dye with the bare eye under normal light. This was not possible for every cylinder, hence some of the fractals appear to be blurry. Some cylinders broke during the cutting process. However, every fractal could be recovered and an image acquired. Cylinder 3 broke apart during the cutting process [Figure 24]. All of the 3 gels (gel 1-3) showed blurry fractals, what were interpret as the central cross section not being optimally cut out of the cylinder in the right plane. Nevertheless, the fractals' structure can be recognized in each of the gels. A repetition of these gels with the correct plane of cutting the cylinder might give better results.

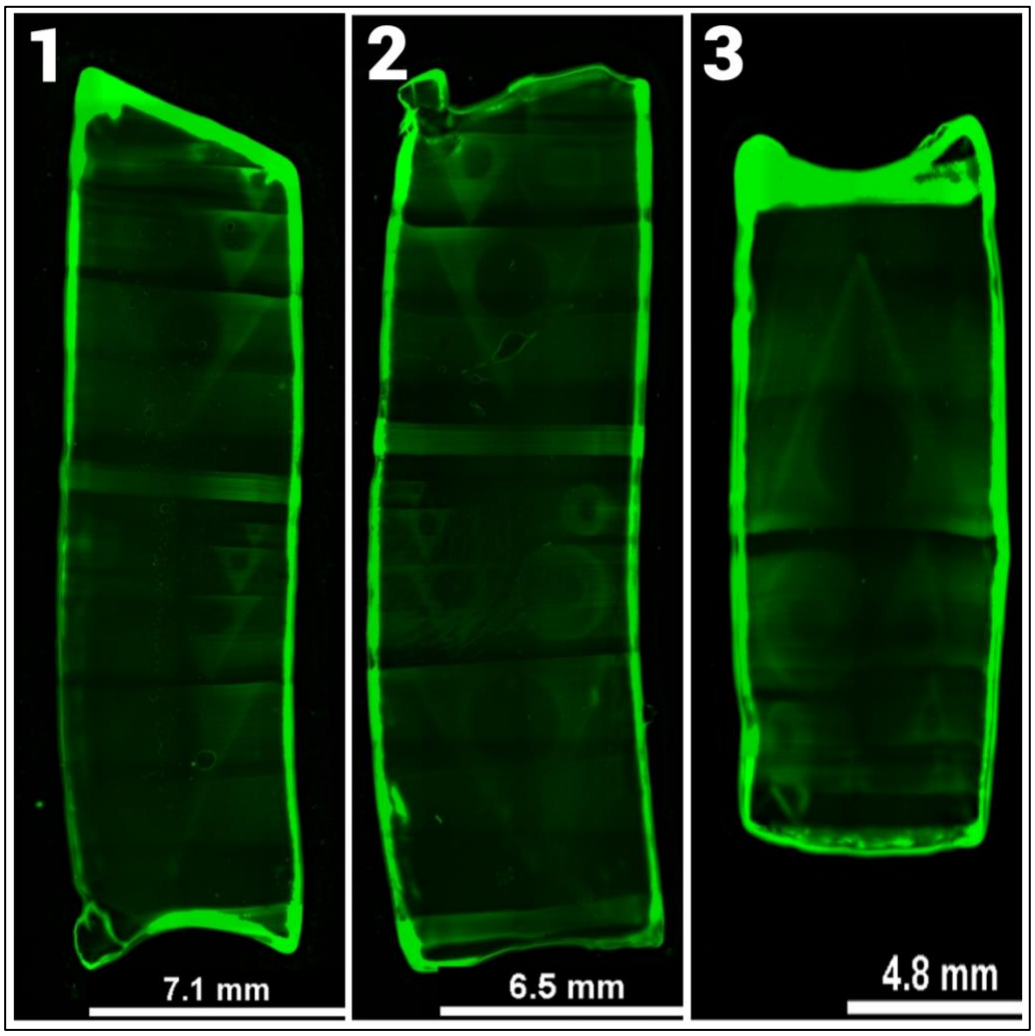

Figure 24: 6.3.2 Grafting optimization – *Picture of gel 1,2 and 3 of the fractal grafting experiment to optimize the grafting conditions. The hydrogel cylinders had a concentration of 5% w/v GelNOR and were crosslinked with 4.2mM DTT and 0.05% w/v LAP in an UV-Oven for 10 minutes. PEG-Cy3 was used as a fluorescent dye. The varying conditions between the cylinders were concentration of LAP and TEMPO, the cylinders were infused with. The lower fractals were printed with a light dose of 2000 mJ/cm². The upper fractals were printed with a light dose of 4000 mJ/cm² and solely serve the purpose of the identification of the correct cutting plane.*

The fractal in cylinder 4 showed a blurry structure without sharp forms [Figure 25]. This is likely to be the effect of choosing the wrong plane to cut the cross section out of the hydrogel cylinder. The data retrieved from this cylinder can be seen as invalid and a repetition of the experiment for this cylinder might be needed. Cylinder 5, however, showed a clear structure of the fractals being grafted into the hydrogel. The upper fractal shows areas of high intensity in the signal in the first circular structure. This is not surprising, as the upper fractal was printed with a light dose 4000 mJ/cm^2 and solely served the purpose of identifying the correct plane to cut the central cross section out of the hydrogel cylinder. The lower fractal, on the other hand, shows a clear structure of the intended grafting template. Even the smallest triangle on the top can be recognized including the central hole. This triangle had a size of 0.875 mm. Horizontal bands can be seen going through the cylinder. This was the case

where the printed structure shows a certain width and therefore, the lowest parts of the triangles and the lower parts of the holes in the structures did not show these bands. This is interpreted as unspecific grafting, where the width of the fractal surpasses a certain threshold. Cylinder 6 showed a similarly grafted fractal, but with areas of high signal in the first 2 fractal planes (from bottom to top). The smallest triangle in the top middle was also present, as well as the horizontal bands of unspecific grafting. Therefore, the grafting resolution can be seen to be in the range of approximately 875 μm. Comparing this grafting resolution with the previously mentioned two photon patterning process by Broguiere et al., who could patternize fluorescein with a resolution of 2-40 μm into various hydrogel matrices, this resolution seemingly falls behind. However, the constructs grafted by Broguiere et al. just had a size of <1mm and therefore no significant size scalability fitting the means of a medical application (39). Additionally, these experiments served as a proof of concept for the grafting of bioactive molecules into GelNOR hydrogels in a spatially controlled fashion, which is proven to be possible. Further research will certainly improve the resolution of the grafting process, which will propel the advancements of VBP, due to its fast pace and manifold application possibilities.

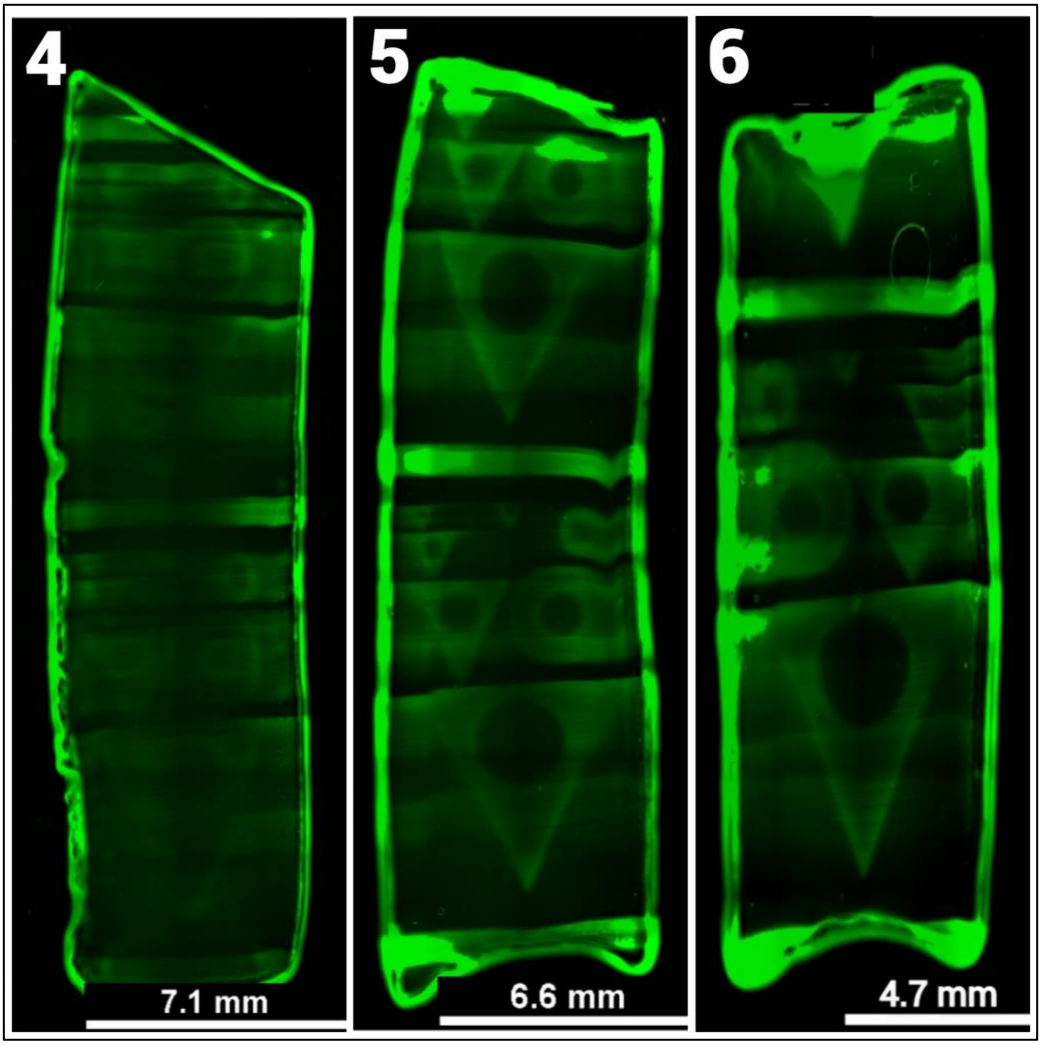

Figure 25: 6.3.2 Grafting optimization – *Picture of gel 4,5 and 6 of the fractal grafting experiment to optimize the grafting conditions. The hydrogel cylinders had a concentration of 5% w/v GelNOR and were crosslinked with 4.2mM DTT and 0.05% w/v LAP in an UV-Oven for 10 minutes. PEG-Cy3 was used as a fluorescent dye. The varying conditions between the cylinders were concentration of LAP and TEMPO, the cylinders were infused with. The lower fractals were printed with a light dose of 2000 mJ/cm². The upper fractals were printed with a light dose of 4000 mJ/cm² and solely serve the purpose of the identification of the correct cutting plane.*

To further assess the resolution of the grafted fractals, Ratio1-3 for the grafted fractals were calculated [Table 8]. In these calculations, the average signal intensity of the bottom triangle (without the hole) was used as a value instead of the disc intensity, the average intensity of the hole of the bottom triangle as the intensity of the sides, and finally the average intensity of the section below the central crossbar between the fractals as background. Ratio1 shows an average value of 2.1335 with a relative standard deviation of 44.5%. Ratio2 has an average value of 1.1565 and a relative standard deviation of 12.0%. The results of Ratio3 average at 1.8219, showing a relative standard deviation of 39.4%. With big parts of the underlying data being invalid, the statistical analysis lacks meaningfulness. With the repetition of the experiment and the acquisition of valid data, the statistical analysis would gain expressiveness.

Gel	LAP [w/v%]	TEMPO [w/v%]	Light dose [mJ/cm²]	Ratio1	Ratio2	Ratio3
1	0.8	0.007	2000	1.3372	0.9149	1.4616
2	0.8	0.008	2000	1.4554	1.1609	1.2537
3	0.8	0.009	2000	1.9368	1.0795	1.7941
4	1.0	0.007	2000	1.3333	1.2152	1.0972
5	1.0	0.008	2000	2.8333	1.3684	2.0705
6	1.0	0.009	2000	3.9048	1.2000	3.2540

Table 8: 6.3.2 Grafting optimization – *Calculated values for ratio1-3 and the respective grafting conditions of the fractals for the fractal grafting experiment to optimize the grafting conditions. The hydrogel cylinders had a concentration of 5% w/v GelNOR and were crosslinked with 4.2mM DTT and 0.05% w/v LAP in an UV-Oven for 10 minutes. PEG-Cy3 was used as a fluorescent dye. The varying conditions between the cylinders were concentration of LAP and TEMPO, the cylinders were infused with. The light dose, used to graft the fractals, was 2000 mJ/cm².*

Despite being grafted under similar conditions, the fractals of gel 5 and 6 gave significantly different results for Ratio1-3. This can be explained by the fact, that the fractal of gel 6 had a significantly lower signal intensity in the triangles hole. This is interpreted to be an effect of the higher concentration of TEMPO. Due to this, the values for Ratio1-3 differ a lot between the two fractals. However, the grafting resolution for both cylinders are considered to be good. A repetition of gel 1 to 4 should be carried out to further improve the results of this experiment.

7 Conclusion

This work described the synthesis and analysis of GelNOR with a high DOF of 88% in average, in order to utilize it for further modification. Furthermore, the bioinks printing properties were assessed, including the identification of printing parameters, influencing the printing resolution. The most influencing parameters on the printing resolution identified are the concentration of PI, the crosslinking molecule and the photo inhibitor in the bioink, as well as the light dose used during the printing process. Most importantly, a method to graft biological molecules into GelNOR hydrogels in a volumetric printing process was not only proven to be feasible, but also characterized by identifying parameters, responsible for the spatially controlled grafting with resolution. Similar to the printing of GelNOR, the grafting resolution was mostly correlated to the concentration of the PI and a photo inhibitor in addition to the light dose. There is no evidence, that this method of grafting has been characterized or even done by research groups before, providing novelty to this work. This work lays the foundations for the printing of specialized tissue with GelNOR, thereby representing a quantum leap for biofabrication and especially volumetric bioprinting.

8 Future work

After this first assessment of the properties, possibilities and limits of GelNOR, a set of subsequent experiments would help to further characterize this material:

A question, not answered by this report, is the rigidity and elasticity of the hydrogels. Therefore, rheological measurements with various concentrations of GelNOR, LAP and DTT can be performed, to further assess the physical properties of the hydrogel. Similar experiments were carried out by Rizzo et al. (25). However, the synthesized GelNOR by Rizzo et al. had a lower DOF than the material in this report. This difference in combination with a lower saturation degree of norbornene groups with thiol groups and the use of DTT as a crosslinker will most likely result in a different hydrogel stiffness. It is to expect, that a significantly higher DOF, in combination with a weaker crosslinker (DTT instead of PEG4SH) and a lower degree of norbornene saturation, will result in similar physical properties. But of course, this remains to be tested.

An experiment of this report, that was carried out to test the grafting resolution on a three-dimensional structure [Figure 26], was based on the results of the previous experiments of the fractal grafting.

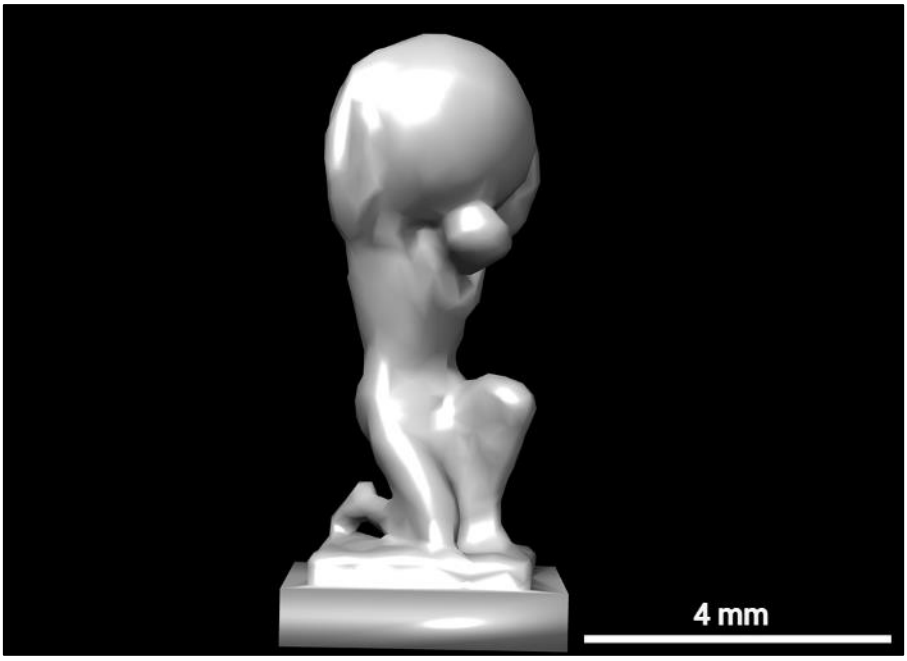

Figure 26: 8 Future work – *Three-dimensional figure of Atlas holding the world used for the grafting experiment of a three-dimensional construct. The structures height is approximately 8mm.*

Unfortunately, the grafted hydrogel cylinders decayed during the storage before the image acquisition, despite being stored in PBS which contained sodium azide. If this was caused by a microbial infection or merely by a decay over time is yet to be determined. This experiment could not be repeated due to timely matters but would add crucial insights to this report.

A possibility to increase the properties and possibilities of GelNOR is to substitute DTT with other molecules with two or even more thiol groups as a crosslinker. These molecules could have a smaller or larger distance between their thiol groups in order to control the hydrogel's mesh size. Analogue to Rizzo et al. and Greene et al., PEG4SH [Figure 8] could be used as a crosslinker, but with the same norbornene saturation degree of 70% (25,28). It is plausible, that this would result in hydrogels with a higher shape fidelity, as one crosslinker molecule serves as a junction knot for 4 norbornene groups (25). Thereby, stronger gels can be printed, while simultaneously retaining a certain amount of norbornene groups for further modification. Additionally, it could be possible to attach one or more functional groups to these new crosslinkers to add a whole variety of possibilities to them.

Another essential component of a hydrogel for volumetric bioprinting is the cytocompatibility. Do cells survive the printing process, is the material cytotoxic, does the hydrogel allow cell attachment and can cells proliferate in the material? As mentioned above, Greene et al. conducted a set of experiments, in which they could prove the high cytocompatibility of GelNOR (28). What is still to be researched is the cytocompatibility of hydrogels with a norbornene saturation of below 100%. A set of experiments entailing the printing of GelNOR with a saturation degree of approximately 70%, containing cells and the following cultivation of the hydrogel could give insights to these questions.

After proving the concept of grafting biological molecules (BSA) into a GelNOR hydrogel, the questions of their biological activity, remains. A possible way to assess the biological activity of the grafted molecules is the grafting of chemokines onto one half of a hydrogel and later incubating leukocytes on the gel. Chemokines are a group of proteins, that promote the migration of leukocytes as an inflammatory response (41). In case of the grafted chemokines still being biologically active, the leukocytes would migrate to the grafted side of the hydrogel. A possible candidate for the grafting is the chemokine Macrophage Inflammatory Protein 1α (MIP-1α), as it promotes the migration of monocytes (42).

A further set of experiments to massively widen the possible applications of GelNOR could be the development of a method, that allows the grafting of molecules without a free thiol-group. This could be achieved by developing a peptide linker, that can be linked to a protein. An essential component for this peptide sequence is a grafting region containing cysteines, in order to enable the grafting of the modified molecule. A question that goes along with such experiments is the functionality of these modified molecules. Another possible feature of the peptide linker could be a "cleavable" region, allowing the cells within the hydrogel to detach and ingest the grafted molecules. Obviously, the question of those modified molecules' activity after the cellular ingestion remains to be investigated too. Similar experiments have been carried out by Batalov et al. who were able to crosslink fluorescent proteins into hydrogels based on collagen and fibrin, by modifying the proteins C terminus with a reactive carbonyl group (43). The possibility of grafting all kinds of proteins or other molecules into GelNOR would increase its usefulness even further.

9 References

1. Moroni L, Boland T, Burdick JA, De Maria C, Derby B, Forgacs G, et al. Biofabrication: A Guide to Technology and Terminology. Trends Biotechnol. 2018 Apr 1;36(4):384–402.
2. Bajaj P, Schweller RM, Khademhosseini A, West JL, Bashir R. 3D Biofabrication Strategies for Tissue Engineering and Regenerative Medicine. Annu Rev Biomed Eng. 2014 Jul 11;16:247–76.
3. Zhu N, Chen X. Biofabrication of Tissue Scaffolds [Internet]. Advances in Biomaterials Science and Biomedical Applications. IntechOpen; 2013 [cited 2022 Aug 8]. Available from: https://www.intechopen.com/chapters/undefined/state.item.id
4. Groll J, Burdick JA, Cho DW, Derby B, Gelinsky M, Heilshorn SC, et al. A definition of bioinks and their distinction from biomaterial inks. Biofabrication. 2018 Nov;11(1):013001.
5. Li X, Liu B, Pei B, Chen J, Zhou D, Peng J, et al. Inkjet Bioprinting of Biomaterials. Chem Rev. 2020 Oct 14;120(19):10793–833.
6. Kim SJ, Lee G, Park JK. Direct Microextrusion Printing of a Low Viscosity Hydrogel on a Supportive Microstructured Bioprinting Substrate for the Vasculogenesis of Endothelial Cells. Adv Mater Technol. n/a(n/a):2101326.
7. Pedde RD, Mirani B, Navaei A, Styan T, Wong S, Mehrali M, et al. Emerging Biofabrication Strategies for Engineering Complex Tissue Constructs. Adv Mater. 2017;29(19):1606061.
8. Dou C, Perez V, Qu J, Tsin A, Xu B, Li J. A State-of-the-Art Review of Laser-Assisted Bioprinting and its Future Research Trends. ChemBioEng Rev. 2021;8(5):517–34.
9. Zheng Z, Eglin D, Alini M, Richards GR, Qin L, Lai Y. Visible Light-Induced 3D Bioprinting Technologies and Corresponding Bioink Materials for Tissue Engineering: A Review. Engineering. 2021 Jul 1;7(7):966–78.
10. Grigoryan B, Sazer DW, Avila A, Albritton JL, Padhye A, Ta AH, et al. Development, characterization, and applications of multi-material stereolithography bioprinting. Sci Rep. 2021 Feb 4;11(1):3171.
11. Ozbolat IT, Hospodiuk M. Current advances and future perspectives in extrusion-based bioprinting. Biomaterials. 2016 Jan 1;76:321–43.
12. Bernal PN, Delrot P, Loterie D, Li Y, Malda J, Moser C, et al. Volumetric Bioprinting of Complex Living-Tissue Constructs within Seconds. Adv Mater. 2019;31(42):1904209.
13. Gehlen J, Qiu W, Schädli GN, Müller R, Qin XH. Tomographic volumetric bioprinting of heterocellular bone-like tissues in seconds. Acta Biomater [Internet]. 2022 Jun 16 [cited 2022 Jul 14]; Available from: https://www.sciencedirect.com/science/article/pii/S1742706122003580
14. Loterie D, Delrot P, Moser C. High-resolution tomographic volumetric additive manufacturing. Nat Commun. 2020 Feb 12;11(1):852.
15. Yue K, Trujillo-de Santiago G, Alvarez MM, Tamayol A, Annabi N, Khademhosseini A. Synthesis, properties, and biomedical applications of gelatin methacryloyl (GelMA) hydrogels. Biomaterials. 2015 Dec 1;73:254–71.
16. Bernal PN, Bouwmeester M, Madrid-Wolff J, Falandt M, Florczak S, Rodriguez NG, et al. Volumetric Bioprinting of Organoids and Optically Tuned Hydrogels to Build Liver-Like Metabolic Biofactories. Adv Mater. 2022;34(15):2110054.
17. Lim KS, Galarraga JH, Cui X, Lindberg GCJ, Burdick JA, Woodfield TBF. Fundamentals and Applications of Photo-Cross-Linking in Bioprinting. Chem Rev. 2020 Oct 14;120(19):10662–94.

18. Noshadi I, Hong S, Sullivan KE, Sani ES, Portillo-Lara R, Tamayol A, et al. In Vitro and In Vivo Analysis of Visible Light Crosslinkable Gelatin Methacryloyl (GelMA) Hydrogels. Biomater Sci. 2017 Sep 26;5(10):2093–105.
19. Aromaa MK, Vallittu PK. Delayed post-curing stage and oxygen inhibition of free-radical polymerization of dimethacrylate resin. Dent Mater. 2018 Sep 1;34(9):1247–52.
20. Lee TY, Guymon CA, Jönsson ES, Hoyle CE. The effect of monomer structure on oxygen inhibition of (meth)acrylates photopolymerization. Polymer. 2004 Aug 19;45(18):6155–62.
21. Zhao C, Wu Z, Chu H, Wang T, Qiu S, Zhou J, et al. Thiol-Rich Multifunctional Macromolecular Crosslinker for Gelatin-Norbornene-Based Bioprinting. Biomacromolecules. 2021 Jun 14;22(6):2729–39.
22. Williams D, Thayer P, Martinez H, Gatenholm E, Khademhosseini A. A perspective on the physical, mechanical and biological specifications of bioinks and the development of functional tissues in 3D bioprinting. Bioprinting. 2018 Mar 1;9:19–36.
23. Mũnoz Z, Shih H, Lin CC. Gelatin hydrogels formed by orthogonal thiol–norbornene photochemistry for cell encapsulation. Biomater Sci. 2014;2(8):1063–72.
24. Lin CC, Ki CS, Shih H. Thiol–norbornene photoclick hydrogels for tissue engineering applications. J Appl Polym Sci [Internet]. 2015 [cited 2022 Jul 20];132(8). Available from: https://onlinelibrary.wiley.com/doi/abs/10.1002/app.41563
25. Rizzo R, Ruetsche D, Liu H, Zenobi-Wong M. Optimized Photoclick (Bio)Resins for Fast Volumetric Bioprinting. Adv Mater. 2021;33(49):2102900.
26. Tüdős F, Földes-Berezsnich T. Free-radical polymerization: Inhibition and retardation. Prog Polym Sci. 1989 Jan 1;14(6):717–61.
27. DL-Dithiothreitol (DTT) [Internet]. [cited 2022 Jun 9]. Available from: https://phytotechlab.com/dl-dithiothreitol-dtt.html
28. Greene T, Lin TY, Andrisani OM, Lin CC. Comparative study of visible light polymerized gelatin hydrogels for 3D culture of hepatic progenitor cells. J Appl Polym Sci [Internet]. 2017 Mar 15 [cited 2022 Jul 21];134(11). Available from: https://onlinelibrary.wiley.com/doi/10.1002/app.44585
29. Göckler T, Haase S, Kempter X, Pfister R, Maciel BR, Grimm A, et al. Tuning Superfast Curing Thiol-Norbornene-Functionalized Gelatin Hydrogels for 3D Bioprinting. Adv Healthc Mater. 2021;10(14):2100206.
30. Dobos A, Van Hoorick J, Steiger W, Gruber P, Markovic M, Andriotis OG, et al. Thiol–Gelatin–Norbornene Bioink for Laser-Based High-Definition Bioprinting. Adv Healthc Mater. 2020;9(15):1900752.
31. TNBSA Solution (2,4,6-trinitrobenzene sulfonic acid) (5% w/v) [Internet]. [cited 2022 Jun 8]. Available from: https://www.thermofisher.com/order/catalog/product/cn/zh/28997
32. Elkhoury K, Morsink M, Tahri Y, Kahn C, Cleymand F, Shin S, et al. Synthesis and characterization of C2C12-laden gelatin methacryloyl (GelMA) from marine and mammalian sources. Int J Biol Macromol. 2021 May 1;183.
33. Verification of Photometric Measurement Values at a Glance - Eppendorf Handling Solutions [Internet]. [cited 2022 Apr 19]. Available from: https://handling-solutions.eppendorf.com/sample-handling/photometry/did-you-know/detailview-did-you-know/news/verification-of-photometric-measurement-values-at-a-glance-1/
34. organic-nmr-quick-guide.pdf [Internet]. [cited 2022 Aug 10]. Available from: https://nmrweb.chem.ox.ac.uk/Data/Sites/70/userfiles/pdfs/organic-nmr-quick-guide.pdf
35. PIERCE_ProteinStorage.pdf [Internet]. [cited 2022 Jun 10]. Available from: http://wolfson.huji.ac.il/purification/PDF/StorageProteins/PIERCE_ProteinStorage.pdf

36. Piehl LL, Facorro GB, Huarte MG, Desimone MF, Copello GJ, Díaz LE, et al. Plasmatic antioxidant capacity due to ascorbate using TEMPO scavenging and electron spin resonance. Clin Chim Acta. 2005 Sep 1;359(1):78–88.
37. Luk SB, Azevedo LA, Maric M. Reversible deactivation radical polymerization of bio-based dienes. React Funct Polym. 2021 May 1;162:104871.
38. Siriwardana K, Wang A, Gadogbe M, Collier WE, Fitzkee NC, Zhang D. Studying the Effects of Cysteine Residues on Protein Interactions with Silver Nanoparticles. J Phys Chem C Nanomater Interfaces. 2015;119(5):2910–6.
39. Broguiere N, Lüchtefeld I, Trachsel L, Mazunin D, Rizzo R, Bode JW, et al. Morphogenesis Guided by 3D Patterning of Growth Factors in Biological Matrices. Adv Mater. 2020 Jun;32(25):1908299.
40. Cy3 PEG Thiol, Cy3-PEG-SH [Internet]. [cited 2022 Sep 13]. Available from: http://www.nanocs.net/Cy3-PEG-SH-5k.htm
41. Hughes CE, Nibbs RJB. A guide to chemokines and their receptors. Febs J. 2018 Aug;285(16):2944–71.
42. DiPietro LA, Burdick M, Low QE, Kunkel SL, Strieter RM. MIP-1alpha as a critical macrophage chemoattractant in murine wound repair. [Internet]. American Society for Clinical Investigation; 1998 [cited 2022 Jun 14]. Available from: https://www.jci.org/articles/view/1020/pdf
43. Batalov I, Stevens KR, DeForest CA. Photopatterned biomolecule immobilization to guide three-dimensional cell fate in natural protein-based hydrogels. Proc Natl Acad Sci. 2021 Jan 26;118(4):e2014194118.